

Enhanced spontaneous emission of Bloch oscillation radiation from a single energy band

G. J. Iafrate

*Department of Electrical and Computer Engineering,
North Carolina State University, Raleigh, North Carolina 27695-8617*

Abstract

In this study, we explored the possibility of enhanced spontaneous emission of radiation beyond the free space value by analyzing a semiconductor superlattice structure placed in a microcavity whose resonant modes were tuned to the Bloch frequency. In particular, we considered the spontaneous emission of Bloch radiation into the dominant mode of a rectangular waveguide. In the analysis, the quantum radiation field was described by the waveguide quantized electromagnetic field in the Coulomb gauge, and the instantaneous eigenstates of the Bloch Hamiltonian were used as basis states to analyze the Bloch dynamics to all orders in the constant external electric field. The results predict that the spontaneous emission occurs with frequencies equal to integral multiples of the Bloch frequency without any *ad hoc* assumptions made concerning the existence of Wannier-Stark ladder levels; such quantization effects arise from a natural consequence of the implicit quantum selection rules. It was shown that the power radiated into the dominant mode of a rectangular waveguide can be enhanced by an order of magnitude in comparison with that for the free space spontaneous emission by tuning the Bloch frequency to align with the spectral region of the waveguide spectral density peak. For GaAs-based superlattices, the power radiated from spontaneous emission due to Bloch oscillations in the terahertz frequency range was estimated to be about several microwatts.

REPORT DOCUMENTATION PAGE

Form Approved
OMB NO. 0704-0188

Public Reporting burden for this collection of information is estimated to average 1 hour per response, including the time for reviewing instructions, searching existing data sources, gathering and maintaining the data needed, and completing and reviewing the collection of information. Send comment regarding this burden estimates or any other aspect of this collection of information, including suggestions for reducing this burden, to Washington Headquarters Services, Directorate for information Operations and Reports, 1215 Jefferson Davis Highway, Suite 1204, Arlington, VA 22202-4302, and to the Office of Management and Budget, Paperwork Reduction Project (0704-0188,) Washington, DC 20503.

1. AGENCY USE ONLY (Leave Blank)		2. REPORT DATE 07.25.06	3. REPORT TYPE AND DATES COVERED Final Progress Report 10.01.05 - 06.30.06	
4. TITLE AND SUBTITLE Enhanced spontaneous emission of Bloch oscillation radiation from a single energy band			5. FUNDING NUMBERS W911NF-05-1-0575	
6. AUTHOR(S) Prof. G. J. Iafrate				
7. PERFORMING ORGANIZATION NAME(S) AND ADDRESS(ES) North Carolina State University Research Administration & Sponsored Program Services 2 Leazer Hall Room 1 2230 Stinson Dr. Raleigh, NC, 27695-7514			8. PERFORMING ORGANIZATION REPORT NUMBER	
9. SPONSORING / MONITORING AGENCY NAME(S) AND ADDRESS(ES) U. S. Army Research Office P.O. Box 12211 Research Triangle Park, NC 27709-2211			10. SPONSORING / MONITORING AGENCY REPORT NUMBER 49577.1-EL-II	
11. SUPPLEMENTARY NOTES The views, opinions and/or findings contained in this report are those of the author(s) and should not be construed as an official Department of the Army position, policy or decision, unless so designated by other documentation.				
12 a. DISTRIBUTION / AVAILABILITY STATEMENT Approved for public release; distribution unlimited.			12 b. DISTRIBUTION CODE	
13. ABSTRACT (Maximum 200 words) In this study, we explored the possibility of enhanced spontaneous emission of radiation beyond the free space value by analyzing a superlattice structure placed in a microcavity whose resonant modes were tuned to the Bloch frequency. In particular, we considered the spontaneous emission of Bloch radiation into the rectangular waveguide dominant mode. In the analysis, the quantum radiation field was described by the waveguide quantized electromagnetic field in the Coulomb gauge, and the instantaneous eigenstates of the Bloch Hamiltonian were used as basis states to analyze the Bloch dynamics to all orders in the constant external electric field. The results predict that the spontaneous emission occurs with frequencies equal to integral multiples of the Bloch frequency without any ad hoc assumptions made concerning the existence of Wannier-Stark ladder levels; such quantization effects arise from a natural consequence of the implicit quantum selection rules. It was shown that the power radiated into the dominant mode of a rectangular waveguide can be enhanced by an order of magnitude in comparison with that for the free space spontaneous emission by tuning the Bloch frequency to align with the spectral region of the waveguide spectral density peak. For GaAs-based superlattices, the power radiated from spontaneous emission due to Bloch oscillations in the terahertz frequency range was estimated to be about several microwatts.				
14. SUBJECT TERMS			15. NUMBER OF PAGES 11	
			16. PRICE CODE	
17. SECURITY CLASSIFICATION OR REPORT UNCLASSIFIED	18. SECURITY CLASSIFICATION ON THIS PAGE UNCLASSIFIED	19. SECURITY CLASSIFICATION OF ABSTRACT UNCLASSIFIED	20. LIMITATION OF ABSTRACT UL	

NSN 7540-01-280-5500

Standard Form 298 (Rev.2-89)
Prescribed by ANSI Std. Z39-18
298-102

Enclosure 1

I. Introduction

Electrons in a miniband of a semiconductor superlattice (SL), accelerated by an electric field \mathbf{E} applied in the transverse direction to the SL layers without scattering, can undergo Bloch oscillations¹⁻³ with frequency $\omega_B = eEa/\hbar$, where a is the SL period. The Bloch frequency ω_B can be tuned with external field \mathbf{E} so as to vary from the high gigahertz to the terahertz (THz) frequency range, thus suggesting the applicability of such internal oscillations as a tunable solid-state source for submillimeter wave radiation.² Most recently, Bloch oscillations have been confirmed by using time-domain terahertz emission spectroscopy in GaAs-based SL structures.^{4,5} There have been also a lot of discussions relating the coupling of coherent Bloch oscillations to other fundamental solid-state excitations such as photons,^{6,7} optical phonons,⁸ and plasmons.⁹ In this study, we analyze the spontaneous emission (SE) of radiation resulting from a Bloch electron accelerated by a constant electric field through a miniband of a SL structure placed in a resonance microcavity.

The use of an electromagnetic cavity is well known to maintain resonant conditions at a given frequency to provide a positive suitable feedback in various microwave oscillator schemes¹⁰ as well as in optical¹¹ and terahertz¹² laser systems. An increase of the overall emitted THz power of more than one order of magnitude has been reported by placing a surface-field emitter inside a THz cavity.¹³ As examples relevant to this work, many efforts have been focused on increasing of the SE rate in optical microcavities.¹⁴ The effect of electromagnetic wave confinement (i.e., when at least one dimension of the cavity is of the order of the radiative wavelength) is to redistribute the free-space mode spectral density so as to increase it at some frequencies and to decrease it at others. Therefore, for an active medium in a cavity structure, the SE rate can be enhanced or diminished depending on the position of the emission frequency relative to the cavity-mode spectral density.^{14,15}

II. Bloch oscillator model configuration

We assume that the SL structure is placed into a waveguide with rectangular cross section $L_x \times L_y$ and length L_z , where the coordinate axes are chosen to be along the waveguide edges. The dc electric field \mathbf{E} is applied along the y axis, which is also the SL growth direction. The electromagnetic field inside the waveguide with assumed perfectly conducting walls is determined by the guided modes corresponding to standing waves with respect to the X

and Y axes [designated by an integer pair (m, n)] and propagating waves along the Z axis characterized by propagation constant q_z . Such modes form a complete and orthogonal basis set for describing the electromagnetic fields within the waveguide. In the following, we will consider only transverse electric (TE) modes, where the electric field is perpendicular to the direction of propagation. For practical cases,¹⁶ the most important of all confined modes is the TE₁₀ mode ($m = 1, n = 0$), which is the dominant mode of a waveguide with $L_x > L_y$. This mode has the lowest attenuation and its electric field, \mathbf{E}_r , for the chosen system geometry, is polarized in the direction of the dc field \mathbf{E} . We consider only one excited, TE₁₀, mode while all the other less effective TE and TM modes are ignored. For this mode, we have the following zero electric field $E_{r,x} = E_{r,z} = 0$ and magnetic field $H_{r,y} = 0$ components. Thus, the vector potential \mathbf{A}_r of the field has only one nonzero (y) component, so that

$$A_{r,y} = \sum_{q_z} \sqrt{\frac{4\pi\hbar c^2}{\omega_q \varepsilon V}} \sin(q_x x) (a_q e^{iq_z z} + a_q^\dagger e^{-iq_z z}), \quad (1)$$

where $q_z = 2\pi l/L_z$ (l is an integer), $q_x = \pi/L_x$, c is the velocity of light in vacuum, $V = L_x L_y L_z$ is the waveguide volume, a_q^\dagger and a_q are the creation and annihilation boson operators, and ε is the dielectric constant of the medium filling the waveguide. The normalization constant in Eq. (1) is chosen in such a way that the Hamiltonian for the quantized radiation field has the usual form $H_r = \sum_q \hbar \omega_q a_q^\dagger a_q$, where $\omega_q = \omega_c [1 + (q_z/q_x)^2]^{1/2}$ is the mode dispersion relation, and $\omega_c = q_x c / \sqrt{\varepsilon}$ is the angular cutoff frequency. The guided mode wavelength is written as $\lambda = \lambda_c / [(\omega_q/\omega_c)^2 - 1]^{1/2}$, where $\lambda_c = 2L_x$ is the cutoff wavelength.¹⁰

III. Bloch Hamiltonian and quantum dynamics based on instantaneous eigenstates

In this analysis, the dynamical properties are considered for the situation in which the electron is confined to a single miniband ‘ n_0 ’ of a SL while the effects of interband coupling¹⁷ and electron intraband scattering are ignored. Therefore, the quantum dynamics is described by the time-dependent Schrödinger equation

$$i\hbar \frac{\partial}{\partial t} |\Psi_{n_0}(t)\rangle = H |\Psi_{n_0}(t)\rangle, \quad (2)$$

where the exact Hamiltonian H can be reduced to a sum of the following Hamiltonians $H = H_0 + H_r + H_I$.¹⁸ Here the first two terms represent the Hamiltonian, $H_0(t) =$

$[\mathbf{p} + \mathbf{p}_c(t)]^2/2m_0 + V_c(\mathbf{r})$, for a single electron in a periodic crystal potential $V_c(\mathbf{r})$ interacting with a homogeneous electric field, and the Hamiltonian, H_r , for the cavity mode electromagnetic field. The Hamiltonian $H_I(t) = -(e/m_0c)\mathbf{A}_r \cdot [\mathbf{p} + \mathbf{p}_c(t)]$, for the first-order interaction between the quantum field and the Bloch electron, couples both subsystems H_0 and H_r , and causes transitions between the accelerated Bloch electron states through photon absorption and emission; $\mathbf{p}_c(t) = e \int_{t_0}^t \mathbf{E}(t')dt'$, m_0 is the free electron mass. The total vector potential consists of $\mathbf{A} = \mathbf{A}_c + \mathbf{A}_r$, where \mathbf{A}_c and \mathbf{A}_r describe the external electric field and the cavity mode quantized radiation field, respectively. Below, starting with the total Hamiltonian H , use is made of first-order time-dependent perturbation theory to calculate SE transitions probabilities between states of $H_0 + H_r$ while regarding $H_I(t) \sim \mathbf{A}_r \cdot [\mathbf{p} + \mathbf{p}_c(t)]$ as a perturbation.¹⁹ The solution to $|\Psi_{n_0}(t)\rangle$ of Eq. (2) can be represented in terms of eigenstates of basis states $|\psi_{n_0\mathbf{k}(t)}, \{n_{\mathbf{q},s}\}\rangle = |\psi_{n_0\mathbf{k}(t)}\rangle |\{n_{\mathbf{q},s}\}\rangle$ of the unperturbed Hamiltonian $H_0 + H_r$ as

$$|\Psi_{n_0}(t)\rangle = \sum_{\mathbf{k}} \sum_{\{n_{\mathbf{q},s}\}} A_{\{n_{\mathbf{q},s}\}}(\mathbf{k}, t) |\psi_{n_0\mathbf{k}(t)}, \{n_{\mathbf{q},s}\}\rangle \times \exp \left\{ -\frac{i}{\hbar} \int_{t_0}^t [\varepsilon_{n_0}(\mathbf{k}(t')) + \sum_{\mathbf{q},s} \hbar\omega_q n_{\mathbf{q},s}] dt' \right\}, \quad (3)$$

where the summation over \mathbf{k} is carried out over the entire Brillouin zone, and $\{n_{\mathbf{q},s}\}$ is specified over all possible combinations of photon occupation number $n_{\mathbf{q},s}$ with photon wave vectors \mathbf{q} and polarization $\hat{\varepsilon}_{\mathbf{q},s}$. The instantaneous eigenstates of H_0 are given by¹⁷ $\psi_{n_0\mathbf{k}(t)}(\mathbf{r}, t) = \Omega^{-1/2} e^{i\mathbf{K}\cdot\mathbf{r}} u_{n_0\mathbf{k}(t)}(\mathbf{r}, t)$, where $u_{n_0\mathbf{k}(t)}(\mathbf{r}, t)$ is the periodic part of the Bloch function, $\mathbf{k}(t) = \mathbf{K} + \mathbf{p}_c(t)/\hbar$, and the values of the electron wave vector \mathbf{K} are determined by the periodic boundary conditions of the periodic crystal of volume Ω .

For the one-photon SE, which assumes that initially no photons are present, the probability amplitude in the wave function of Eq. (3) satisfies the initial condition $A_{\{n_{\mathbf{q},s}\}}(\mathbf{k}, t_0) = \{\delta_{n_{\mathbf{q},s},0}\} \delta_{\mathbf{K},\mathbf{K}_0}$ at time $t = t_0$ when the electric field is turned on. Here, \mathbf{K}_0 and $n_{\mathbf{q},s}^0 = 0$ are the initial values of \mathbf{K} and $n_{\mathbf{q},s}$. The probability amplitude for SE, $A_q(\mathbf{k}_0, t)$, is now evaluated in first-order perturbation theory as

$$A_q(\mathbf{k}_0, t) = D(q_x/q)^{1/2} \int_{t_0}^t dt' v_y(\mathbf{k}_0 - \mathbf{q}_j) \times \exp \left\{ -\frac{i}{\hbar} \int_{t_0}^{t'} [\varepsilon_{n_0}(\mathbf{k}_0) - \varepsilon_{n_0}(\mathbf{k}_0 - \mathbf{q}_j) - \hbar\omega_q] dt_1 \right\}, \quad (4)$$

where $D = -i\sqrt{\pi c\alpha/\omega_c\varepsilon V}$, $\alpha = e^2/\hbar c$ is the fine structure constant, $\mathbf{k}_0(t) = \mathbf{K}_0 + \mathbf{p}_c(t)/\hbar$, $\mathbf{q}_j = \{\pm q_x, 0, q_z\}$ with " + " for $j = 1$ and " - " for $j = 2$, and $q = (q_x^2 + q_z^2)^{1/2}$. Then the emission process results in the well-known SE probability

$$P_e^s(t) = \sum_q \sum_{j=1,2} |A_q(\mathbf{k}_0, t)|^2. \quad (5)$$

IV. Quantum selection rule

In evaluating $A_q(\mathbf{k}_0, t)$, we take into account that the external dc field, \mathbf{E} , is along the Y axis; then, it follows that $k_{0y}(t) = K_{0y} + eE(t - t_0)/\hbar$. In taking advantage of the periodic properties of the terms in Eq. (4), $A_q(\mathbf{k}_0, t)$ is evaluated in *clocked* integral multiples of the Bloch period, so that $t = N\tau_B$, where $\tau_B = 2\pi/\omega_B$, the time to traverse one period of the Brillouin zone. The integral in Eq. (4) over time can be replaced by an integral over k_{0y} through the substitution $dt = (\hbar/eE)dk_{0y}$. Then the probability amplitude, at integral multiples of the Bloch period, can be expressed through that over the single Bloch period, τ_B .^{17,18} Thus we obtain

$$|A_q(\mathbf{k}_0, N\tau_B)|^2 = \frac{\sin^2(N\beta_q/2)}{\sin^2(\beta_q/2)} |A_q(\mathbf{k}_0, \tau_B)|^2, \quad (6)$$

where the parameter β_q is given by

$$\beta_q = 2\pi \frac{\omega_q}{\omega_B} + \frac{1}{eE} \int_{K_{0y}}^{K_{0y}+G_y} dk_{0y} [\varepsilon_{n_0}(\mathbf{k}_0) - \varepsilon_{n_0}(\mathbf{k}_0 - \mathbf{q}_j)], \quad (7)$$

and $G_y = 2\pi/a$, the y component of the SL reciprocal-lattice vector.

From Eq. (6), it is seen that the quantity $|A_q(\mathbf{k}_0, N\tau_B)|^2$ will reach its maximum growth value when $\beta_q = 2\pi(m + \delta)$, where m is an integer and $\delta \rightarrow 0$; for this limit, the function $\sin^2(N\beta_q/2)/\sin^2(\beta_q/2) \rightarrow N^2$, i. e., it becomes sharply peaked at the resonances with increasing N . It is clear that this condition for maximum growth establishes the *selection rule*^{17,18} for the photon emission frequency ω_q . Indeed, from the condition $\beta_q = 2\pi m$, it follows from Eq. (7) in the radiative long-wavelength limit ($qa \ll 1$) that one generally has

$$\omega_q = m\omega_B, \quad q_z = q_{zm} \equiv q_x \left[\left(m \frac{\omega_B}{\omega_c} \right)^2 - 1 \right]^{1/2}, \quad (8)$$

the “*Stark ladder*” resonance condition. Note that \mathbf{q} is not collinear with the direction of the applied field \mathbf{E} , then the integral in Eq. (7) does not vanish because of the periodicity of

$\varepsilon_{n_0}(\mathbf{k}_0)$, and contributes to the selection rule. For $\omega_q = \omega_c[1 + (q_z/q_x)^2]^{1/2}$, this corresponds to neglecting a small term $\sim v_\perp/c$ as compared to unity, where v_\perp is the electron velocity perpendicular to the y axis. Thus, the modes that radiate with the highest probability correspond to the fundamental Bloch frequency and its harmonics. This quantization condition is obtained without requiring any assumptions concerning the existence of Wannier-Stark energy states.

V. Spontaneous emission probability and the enhancement factor

The spontaneous emission probability is evaluated at time $t = N\tau_B$, $P_e^s = P_e^s(N\tau_B)$, by substituting $|A_q(\mathbf{k}_0, N\tau_B)|^2$ from Eq. (6) into Eq. (5). The sum over q in Eq. (5) has been replaced by an integral over q , taking into account the TE₁₀ mode density of states and polarization such that $\sum_q(\dots) \rightarrow (L_z/\pi) \int dq(\dots)/[1 - (q_x/q)^2]^{1/2}$. The integral can be evaluated by using the property of the integrand which contains a sharply peaked, symmetric function of q at $q = q_m = (q_x^2 + q_{zm}^2)^{1/2}$ [see Eq. (8)]. Thus, at every node defined by the resonance conditions, the slowly varying function of q in the integrand can be replaced by its value evaluated at $q = q_m$, and then removed from the integral over q ; after that, the remaining integral can be evaluated to obtain

$$P_e^s = N \frac{L_z \omega_B}{L_x \omega_c} \sum_{l=1}^{l_{max}} \sum_{j=1}^2 \frac{|A_{ql}(\mathbf{k}_0, \tau_B)|^2}{[1 - (q_x/ql)^2]^{1/2}}. \quad (9)$$

Here l_{max} follows from $q_{max} = l_{max}(\omega_B/\omega_c)q_x$, and determines the upper limit in the sum over higher Bloch oscillation harmonics.

The analysis for spontaneous emission and radiation characteristics is now developed by considering a SL miniband in the nearest-neighbor tight-binding approximation. The electron miniband energy dispersion is expressed as $\varepsilon_{n_0}(\mathbf{K}) = \varepsilon_{n_0}(0) + \Delta \sin^2(K_y a/2) + \varepsilon_\perp(\mathbf{K}_\perp)$, where $\varepsilon_{n_0}(0)$ is the band edge, Δ is the miniband width, and $\varepsilon_\perp(\mathbf{K}_\perp)$ is the contribution from the perpendicular components of the miniband. The electron velocity, for the given K_y in the y direction, is then given by $v_y(K_y) = v_{max} \sin(K_y a)$, where $v_{max} = a\Delta/2\hbar$ is the maximum velocity in the miniband.

The calculation of P_e^s in Eq. (9) requires the use of $A_q(\mathbf{k}_0, \tau_B)$ in Eq. (4), evaluated at the maximum growth conditions of Eq. (8), that is when $\hbar\omega_q = m\hbar\omega_B$. In addition, the dependence upon \mathbf{q} in Eq. (4) is made explicit by invoking the assumption of photon

long-wavelength limit, which is valid for all periodic potentials of interest, even SLs, where $q \ll \pi/a$. Thus, we find that

$$|A_{q_l}(\mathbf{k}_0, \tau_B)|^2 = \frac{q_x |DI_l|^2}{q_l \omega_B^2}, \quad (10)$$

where $I_l = \int_{-\pi}^{\pi} d\vartheta_k v_y(\vartheta_k) \exp(-il\vartheta_k)$, and $\vartheta_k = k_{0y}a$. For the nearest-neighbor tight-binding approximation, one can find that $I_l = -i\pi v_{max} \delta_{1l}$. The occurrence of the Kronecker symbol, δ_{1l} , allows the contribution of $l = 1$ term only, thereby limiting, within the nearest-neighbor tight-binding approximation, the generation to the fundamental Bloch harmonic. Then it follows from Eq. (9) that

$$P_e^s = 2\alpha N \frac{L_x}{L_y} \frac{v_m^2}{c^2} \frac{\varepsilon^{1/2} \omega_c^2}{\omega_B^2 (1 - \omega_c^2/\omega_B^2)^{1/2}}. \quad (11)$$

In noting that the SE probability of Bloch radiation into free space with fundamental Bloch frequency is given by the expression¹⁸ $P_{fs}^s = (2\pi/3)\alpha N (v_m/c)^2$, we can compare both the probabilities analyzing the ratio

$$\eta \equiv \frac{P_e^s}{P_{fs}^s} = \frac{3L_x \omega_c^2 \varepsilon^{1/2}}{\pi L_y \omega_B^2 [1 - (\omega_c^2/\omega_B^2)]^{1/2}}. \quad (12)$$

In Fig 1, we show the enhancement factor η as a function of the frequency ratio ω_B/ω_c , which determines detuning of the Bloch frequency with respect to the TE₁₀ mode cutoff frequency. The calculations have been carried out for a GaAs-based SL ($\varepsilon = 12.2$) imbedded into a rectangular waveguide with horizontal and vertical dimensions $L_x/L_y = 2$. It is seen from the figure that the enhancement factor η increases with decreasing detuning parameter ω_B/ω_c reaching values over one order of magnitude for the detuning close to 1.

VI. Numerical estimations and discussion

For numerical estimations, we assume a GaAs-based SL structure with the SL lattice parameter $a = 100 \text{ \AA}$, vertical dimension 9 \mu m , and lateral cross section $18 \times 1000 \text{ \mu m}^2$. Also we assume that waveguide is fully filled with the semiconductor material. The electron density in the active region is taken to be $5 \times 10^{16} \text{ cm}^{-3}$. Taking for the SL lowest miniband energy width $\Delta = 20 \text{ meV}$, the maximum group velocity in the miniband is estimated as $v_{max} = 1.6 \times 10^7 \text{ cm/s}$. These parameter magnitudes are close to those of GaAs-based SL structures used to study high-frequency microwave generation.^{2,20,21} Spontaneous emission

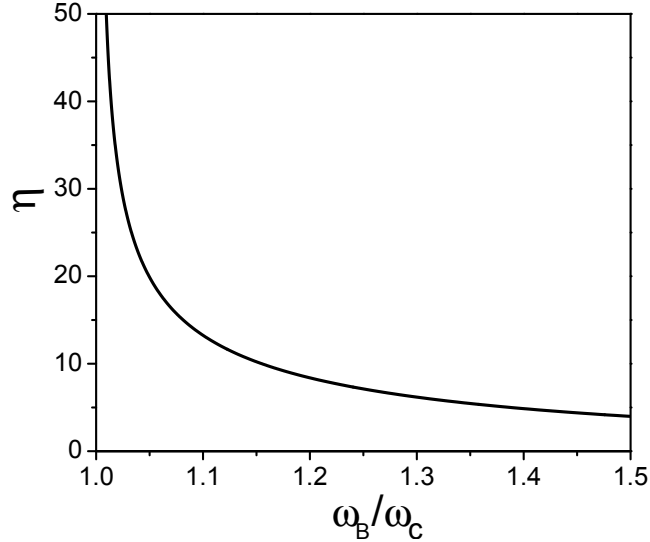


Fig. 1. Enhancement factor η of the spontaneous emission probability as a function of frequency ratio ω_B/ω_c for a GaAs-based SL structure imbedded into a rectangular waveguide.

of a photon with the energy 10 meV corresponds to the Bloch frequency $\nu_B = \omega_B/2\pi = 2.5$ THz. The electric field required to achieve such Bloch frequency is $E = \hbar\omega_B/ea = 10$ kV/cm, and results in the application of nine volts across vertical dimension of the SL structure.²³ The spontaneous emission probability of radiation into free space can be estimated taking, for example, $N = 100$ as $P_{fs}^s = 4.3 \times 10^{-7}$; and the generation energy per electron $\hbar\omega_B P_{fs}^s = 4.3 \times 10^{-6}$ meV. Since there is a total of $n = 8 \times 10^9$ electrons in the active region of the SL, the generated energy achievable is estimated to be $P_{fs} = n\hbar\omega_B P_{fs}^s = 34.4$ eV, which corresponds to a power output generated into free space $W_{fs} = (\nu_B/N)P_{fs} \simeq 0.14 \mu\text{W}$. Although the power generated into free space is discernibly low for the SE of Bloch oscillation radiation, it follows from Eq. (12) that SE probabilities and rates are substantially modified for the case of radiation into the waveguide mode. We find from Fig. 1 that $\eta = 20$, if we take for the detuning parameter $\omega_B/\omega_c = 1.05$. Then, using the obtained value for the enhancement factor, we estimate the power output generated into the TE₁₀ waveguide mode as $W_{wg} \simeq 3 \mu\text{W}$.

It is noted that a Bloch oscillation SL does not require controlled inversion population between Wannier-Stark ladder levels to get the desired SE photon frequency; the desired frequency is controlled by the applied field. Whereas in other SL light generating devices,

such as quantum cascade lasers, a large inversion population is required to provide stimulated emission with resulting high threshold current densities and high heat dissipation. In this regard, the Bloch oscillator in SE offers a novel option for operating at THz frequencies, provided the power output can be enhanced in the coherent Bloch regime. Future directions of this work include the study of limiting factors of electron dephasing due to scattering inhomogeneities in the SL to determine an optimum power enhancement and the efficiency of power extraction from the cavity.

VII. Summary of the most important results

- The quantum electron dynamics and spontaneous emission of radiation for a Bloch electron traversing a single energy miniband of a SL structure in a constant electric field and in the presence of a resonant cavity have been analyzed. The analysis is based on the use of instantaneous eigenstates of the Bloch Hamiltonian good to all orders of the dc field, and to first-order perturbation theory in the quantized radiation field.
- The analysis results in the quantum selection rule which shows that the spontaneous emission into the waveguide dominant mode is sharply peaked at frequencies equal to integral multiples of the Bloch frequency. This result has made use of no *ad hoc* assumptions about the existence of Wannier-Stark quantized energy levels within the band.
- The spontaneous emission probabilities are substantially enhanced in comparison with spontaneous emission into free space when the Bloch frequency is tuned by the field into the spectral peak of the waveguide mode density of states.
- The set of controlling parameters has been specified and their magnitudes have been estimated for the enhanced spontaneous emission due to Bloch oscillations in the terahertz frequency range.
- The enhancement factor has been analyzed as a function of the Bloch frequency and the external electric field. A theoretical estimate of the enhancement factor provides an order of magnitude enhancement for GaAs-based superlattices, and resulted in a power output of $\simeq 3\mu\text{W}$.

-
- ¹ F. Bloch, Z. Phys. **52**, 555 (1928); C. Zener, Proc. R. Soc. London A**145**, 523 (1934); G. H. Wannier, Phys. Rev. **117**, 432 (1960).
- ² L. Esaki and R. Tsu, IBM J. Res. Dev. **14**, 61 (1970).
- ³ For a review see, for instance, K. Leo, Semicond. Sci. Technol. **13**, 249 (1998).
- ⁴ C. Waschke, H. G. Roskos, R. Schwedler, K. Leo, and H. Kurz, and K. Köhler, Phys. Rev. B **70**, 3319 (1993).
- ⁵ Y. Shimada, K. Hirakawa, M. Odnoblioudov, and K. A. Chao, Phys. Rev. Lett. **90**, 046806 (2003).
- ⁶ K. Unterrainer, B. J. Keay, M. C. Wanke, S. J. Allen, D. Leonard, G. Medeiros-Ribeiro, U. Bhattacharya, and M. J. W. Rodwell, Phys. Rev. Lett. **76**, 2973 (1996).
- ⁷ S. Vinnerl, E. Schomburg, S. Brandl, O. Kus, K. F. Renk, M. C. Wanke, S. J. Allen, A. A. Ignatov, V. Ustinov, A. Zhukov, and P. S. Kop'ev, Appl. Phys. Lett. **77**, 1259 (2000).
- ⁸ T. Dekorsy, A. Bartels, H. Kurz, K. Köhler, R. Hey, and K. Ploog, Phys. Rev. Lett. **85**, 1080 (2000).
- ⁹ A. W. Ghosh, L. Jönsson, and J. W. Wilkins, Phys. Rev. Lett. **85**, 1084 (2000).
- ¹⁰ N. Marcuvitz, *Waveguide Handbook* (Peregrinus, London, 1993).
- ¹¹ O. Svelto, *Principle of Lasers* (Fourth Edition, Plenum Press, New York, 1998).
- ¹² L. Mahler, A. Tredicucci, R. Köhler, F. Beltram, H. E. Beere, E. H. Linfield, and D. A. Ritchie, Appl. Phys. Lett. **87**, 181101 (2005).
- ¹³ C. Janke, P. H. Bolivar, A. Bartels, H. Kurz, and H. Künzel, Phys. Rev. B **67**, 155206 (2003); M. Zedler, C. Janke, P. H. Bolivar, H. Kurz, and H. Künzel, Appl. Phys. Lett. **83**, 4196 (2003).
- ¹⁴ In *Spontaneous Emission and Laser Oscillation in Microcavities*, edited by H. Yokoyama and K. Ujihara (CRC Press, Boca Raton, 1995).
- ¹⁵ E. Yablonovitch, Phys. Rev. Lett. **58**, 2059 (1987).
- ¹⁶ G. Gallot, S. P. Jamison, R. W. McGowan, and D. Grischkowsky, J. Opt. Soc. Am. B **17**, 851 (2000).
- ¹⁷ J. B. Krieger and G. J. Iafrate, Phys. Rev. B **33**, 5494 (1986); G. J. Iafrate and J. B. Krieger, *ibid.* **40**, 6144 (1989).
- ¹⁸ V. N. Sokolov, L. Zhou, G. J. Iafrate, and J. B. Krieger, Phys. Rev. B **73**, 205304 (2006).

- ¹⁹ J. Singh, *Quantum Mechanics: Fundamentals and Applications to Technology* (A Wiley-Interscience Publication, New York, 1997), p. 337.
- ²⁰ E. Schomburg, T. Blomeier, K. Hofbeck, J. Grenzer, S. Brandl, I. Lingott, A. A. Ignatov, K. F. Renk, D. G. Pavel'ev, Yu. Koschurinov, B. Ya. Melzer, V. M. Ustinov, S. V. Ivanov, A. Zhukov, and P. S. Kop'ev, *Phys. Rev. B* **58**, 4035 (1998).
- ²¹ A. M. Bouchard and M. Luban, *Phys. Rev. B* **47**, R6815 (1993).
- ²² To prevent charge domain formation that may be possible through negative differential conductance a superstructure of SLs of suitable lengths can be designed. ²³
- ²³ P. G. Savvidis, B. Kolasa, G. Lee, S. J. Allen, *Phys. Rev. Lett.* **92**, 196802 (2004).

Accomplishments from this research

1. V. N. Sokolov, L. Zhou, G. J. Iafrate, and J. B. Krieger, *Spontaneous emission of Bloch oscillation radiation from a single energy band*, *Phys. Rev. B* **73**, 205304 (2006).
2. V. Sokolov, G. Iafrate, and J. Krieger, *Spontaneous emission from accelerated Bloch electrons - Bloch oscillation radiation*. 2006 APS March Meeting (March 13-17, 2006; Baltimore, MD), Session N 17: Focus Session: Semiconductors for THz and IR I; Abstract N 17.00003.
3. V. N. Sokolov, G. J. Iafrate, and J. B. Krieger, *Microcavity enhancement of spontaneous emission for Bloch oscillations*, submitted to *Phys. Rev. B* (Brief Reports) (2006).

Session N17: Focus Session: Semiconductors for THz and IR I

8:00 AM–10:36 AM, Wednesday, March 15, 2006
Baltimore Convention Center - 313

Sponsoring Unit: FIAP
Chair: K. K. Choi, Army Research Laboratory

Abstract: N17.00003 : Spontaneous emission from accelerated Bloch electrons -- Bloch oscillation radiation

8:48 AM–9:00 AM

Preview Abstract

Authors:

Valeriy Sokolov

Gerald Iafrate

(Dept. of Electrical and Computer Engineering, NCSU, Raleigh, NC 27695-8617)

Joseph Krieger

(Dept. of Physics, Brooklyn College, CUNY, Brooklyn, NY 11210)

A theory of spontaneous emission of radiation for a Bloch electron traversing a single band in an external electric field is presented. The radiation field is described by a free space quantized electromagnetic field in the Coulomb gauge. It is shown that the spontaneous emission occurs with frequencies equal to integral multiples of the Bloch frequency without any *ad hoc* assumptions concerning the existence of Wannier-Stark levels. An explicit expression for the transition probability is derived in first-order perturbation theory relative to the radiation field. Although the output frequency of the radiation can be operationally tuned from the gigahertz to terahertz spectral range by varying the constant electric field, it is estimated that a spontaneous emission power output of only about 0.1 of a microwatt is available using GaAs-based superlattices. In this regard, it is noted that the atomic spontaneous emission probability and related transition rates can be enhanced by properly tailoring the surrounding electromagnetic environment. Therefore, considering Bloch oscillations in a resonant microcavity to enhance the spontaneous emission is a noteworthy alternative for exploring tunable gigahertz to terahertz radiation sources.

Spontaneous emission of Bloch oscillation radiation from a single energy band

V. N. Sokolov,* L. Zhou,† and G. J. Iafrate

Department of Electrical and Computer Engineering, North Carolina State University, Raleigh, North Carolina 27695-8617, USA

J. B. Krieger

Department of Physics, Brooklyn College, CUNY, Brooklyn, New York 11210, USA

(Received 18 December 2005; revised manuscript received 8 March 2006; published 2 May 2006)

A theory for the spontaneous emission of radiation for a Bloch electron traversing a single energy band under the influence of a constant external electric field is presented. The constant external electric field is described in the vector potential gauge. The quantum radiation field is described by the free space quantized electromagnetic field in the Coulomb gauge. The instantaneous eigenstates of the Bloch Hamiltonian are introduced as basis states to analyze the Bloch dynamics to all orders in the constant external electric field. The radiation field described by the quantized electromagnetic field provides the vacuum fluctuations that are responsible for the spontaneous emission of radiation of the single electron from the upper regions of the energy band. It is shown that the spontaneous emission occurs with frequencies equal to integral multiples of the Bloch frequency without any *ad hoc* assumptions made concerning the existence of Wannier-Stark ladder levels. An explicit expression for the spontaneous emission transition probability is derived to first order in the quantized radiation field; results show the explicit dependence upon the electron energy band structure, photon polarization, and the directionality of the radiation output. As an illustration, spontaneous emission probabilities are developed and illustrated for nearest-neighbor tight-binding and more realistic superlattice band structure models. For the GaAs-based superlattices, the power radiated into free space from spontaneous emission due to Bloch oscillations in the terahertz frequency range is estimated to be about one-tenth of a microwatt.

DOI: [10.1103/PhysRevB.73.205304](https://doi.org/10.1103/PhysRevB.73.205304)

PACS number(s): 73.63.Hs, 72.10.Bg, 73.21.Cd, 73.50.Mx

I. INTRODUCTION

Bloch electron dynamics in electric fields has been a subject of great interest dating back to the early development of solid-state physics.^{1–3} More recently, the availability of band-engineered superlattices (SLs) and tailored periodic structures has stimulated further activities^{4–15} in electric field-mediated transport and optical absorption in low-dimensional SLs and quantum-well (QW) structures, where bandgaps and bandwidths are typically several orders of magnitude smaller than those of bulk solids. In particular, recent attention has been focused on Bloch oscillations, the \mathbf{k} -space oscillatory behavior afforded to Bloch electrons when moving in a periodic energy band under the influence of a constant electric field in the absence of scattering. For a biased semiconductor SL, the Bloch frequency^{1–4} for such an oscillation is given by $\omega_B = eEa/\hbar$, where E is the applied constant field and a is the SL period; it is evident that the Bloch frequency can be tuned with changing the external electric field so as to vary from the high gigahertz to the terahertz frequency range, thus suggesting the applicability of such internal oscillations as a tunable source for submillimeter wave radiation.⁴

It is interesting to note that transport experiments suggest only indirect⁵ evidence for the manifestation of Bloch oscillations, whereas optical experiments using semiconductor SLs have allowed direct observations.^{6,7} There have been also numerous discussions relating the coupling of coherent Bloch oscillations to other fundamental solid-state excitations such as photons,^{8,9} optical phonons,¹⁰ and plasmons.¹¹ In this paper, in noting that Bloch oscillations might provide a noteworthy alternative for exploring tunable radiation

sources in the gigahertz to terahertz frequency range, a study is undertaken to analyze the spontaneous emission (SE) of radiation resulting from a Bloch electron accelerating through a single band under the influence of a constant external electric field while subject to vacuum field fluctuations.

In the general framework of this work, attention is focused on the theory for the SE of radiation for a Bloch electron traversing a single energy band in a constant external electric field. It is shown that in a *scattering free environment and in fields low enough to ignore interband tunneling*, spontaneous photon emission occurs as the Bloch electron interacts with the quantum radiation field; the emission occurs only with frequencies equal to integral multiples of the Bloch frequency, even though no *ad hoc* assumptions are made concerning the existence of Wannier-Stark levels. The transition probability is found as an explicit function of the electron energy band structure, photon polarization, and directionality of the radiation output.

In Sec. II, the Hamiltonian for a Bloch electron in the quantum electrodynamic field of interest is developed. The classical external electric field is described in the vector potential gauge, and the free space quantized electromagnetic radiation field is treated using the Coulomb gauge. In neglecting the higher-order quantum field-field interaction term, it is shown that the total Hamiltonian reduces to the sum of three contributions, the Hamiltonian for the Bloch electron in the classical external electric field, the Hamiltonian for the free space quantized radiation field, and the Hamiltonian for the first-order interaction between the quantum field and the Bloch electron. In Sec. III, the instantaneous eigenstates of the Bloch Hamiltonian, known as accel-

erated, field-dependent crystal momentum states, are developed.¹⁵ These instantaneous eigenstates are utilized as basis states in describing the time development, and in calculating the SE transition rates of the accelerated Bloch electrons under the action of the perturbing quantum radiation field. In Sec. IV, the polarization properties of the SE resulting from Sec. III are analyzed. Numerical estimates for power generated using a realistic band structure are given. In Sec. V, a summary of overall results is given; also a discussion of key physical issues relevant to Bloch oscillation dephasing is put forth, issues that were set aside in the analysis of this paper, but that need to be considered in future work on this subject. Also, in Appendix A we provide details of the time-dependent perturbation analysis used to calculate transition rates; in Appendix B we provide the calculation of matrix elements utilized in the perturbation calculations of Appendix A.

II. BLOCH HAMILTONIAN IN AN ELECTROMAGNETIC FIELD

The Hamiltonian for a single electron in a periodic crystal potential subject to an external homogeneous electric field of arbitrary strength in a time-varying electromagnetic field is

$$H = \frac{1}{2m_0} \left(\mathbf{p} - \frac{e}{c} \mathbf{A} \right)^2 + V_c(\mathbf{r}) + H_r. \quad (1)$$

Here, $V_c(\mathbf{r})$ is the periodic crystal potential, \mathbf{A} is the total vector potential consisting of $\mathbf{A} = \mathbf{A}_c + \mathbf{A}_r$, and H_r is the Hamiltonian for the free electromagnetic field; \mathbf{p} is the momentum operator, \mathbf{r} is the spatial coordinate, m_0 is the free electron mass, and c is the velocity of light in vacuum. For the vector potential terms, $\mathbf{A}_c(t)$ is the vector potential describing the external electric field. For a homogeneous electric field $\mathbf{E}(t)$, turned on at initial time $t=t_0$, the vector potential is $\mathbf{A}_c(t) = -c \int_{t_0}^t \mathbf{E}(t') dt'$; in addition, letting $\mathbf{F}(t) = e\mathbf{E}(t)$ and $\mathbf{p}_c(t) = \int_{t_0}^t \mathbf{F}(t') dt'$, it then follows that $\mathbf{p}_c(t) = -(e/c)\mathbf{A}_c(t)$. The vector potential term, \mathbf{A}_r , corresponding to the free quantized radiation field, is given as

$$\mathbf{A}_r = \sqrt{\frac{2\pi\hbar c}{V}} \sum_{\mathbf{q},j} \frac{\hat{\mathbf{e}}_{\mathbf{q},j}}{\sqrt{q}} (a_{\mathbf{q},j} e^{i\mathbf{q}\cdot\mathbf{r}} + a_{\mathbf{q},j}^\dagger e^{-i\mathbf{q}\cdot\mathbf{r}}), \quad (2)$$

where $\hat{\mathbf{e}}_{\mathbf{q},j}$ is a unit polarization vector for the radiation mode with wave vector \mathbf{q} and polarization j , and $\hat{\mathbf{e}}_{\mathbf{q},j} \cdot \hat{\mathbf{e}}_{\mathbf{q},j'} = \delta_{jj'}$ with $j, j' = 1, 2$. $a_{\mathbf{q},j}^\dagger$ and $a_{\mathbf{q},j}$ are the creation and annihilation boson operators of the quantum radiation field, V is the volume of the system, and $q = |\mathbf{q}|$, the magnitude of wave vector \mathbf{q} . \mathbf{A}_r satisfies the Coulomb gauge, that is, $\nabla \cdot \mathbf{A}_r = 0$, which means, from Eq. (2), that

$$\hat{\mathbf{e}}_{\mathbf{q},j} \cdot \mathbf{q} = 0, \quad (3)$$

for each polarization direction. It also follows from the Coulomb gauge that $[\mathbf{p}, \mathbf{A}_r] = 0$. The Hamiltonian for the free quantized radiation field is

$$H_r = \sum_{\mathbf{q},j} \hbar \omega_{\mathbf{q}} a_{\mathbf{q},j}^\dagger a_{\mathbf{q},j}, \quad (4)$$

where $\omega_{\mathbf{q}} = cq$, the free space photon dispersion.

In substituting the vector potential $\mathbf{A} = \mathbf{A}_c + \mathbf{A}_r$ into Eq. (1), and regarding the term containing \mathbf{A}_r as a perturbation,¹⁶ we can reduce the total Hamiltonian of Eq. (1) to

$$H = H_0 + H_r + H_I, \quad (5)$$

where

$$H_0(t) = \frac{1}{2m_0} [\mathbf{p} + \mathbf{p}_c(t)]^2 + V_c(\mathbf{r}), \quad (6)$$

and

$$H_I(t) = -\frac{e}{m_0 c} \mathbf{A}_r \cdot [\mathbf{p} + \mathbf{p}_c(t)], \quad (7)$$

where H_r is given by Eq. (4). Equation (5) follows from Eq. (1) in the limit of a low intensity radiation field, where we have dropped the term of order \mathbf{A}_r^2 .¹⁷ In Eq. (5), the first two terms represent the Hamiltonian, $H_0(t)$, for a single electron in a periodic crystal potential interacting with a homogeneous electric field, and the Hamiltonian, H_r , for the free electromagnetic field; the term $H_I(t)$ in Eq. (5), and specified in Eq. (7), couples both subsystems H_0 and H_r , and causes transitions between the accelerated Bloch electron states through photon absorption and emission. In the next section, starting with the total Hamiltonian of Eq. (5), use is made of first-order time-dependent perturbation theory to calculate SE transition probabilities between states of $H_0 + H_r$ while regarding $H_I(t)$ as a perturbation.

III. QUANTUM DYNAMICS BASED ON INSTANTANEOUS EIGENSTATES

A. Crystal Hamiltonian and instantaneous eigenstates

In this analysis, the dynamical properties are considered for the situation in which the electron is confined to a single band “ n_0 ” of a periodic crystal with energy $\varepsilon_{n_0}(\mathbf{K})$; the effects of interband coupling¹⁵ and electron intraband scattering are ignored. Therefore, the quantum dynamics is described by the time-dependent Schrödinger equation,

$$i\hbar \frac{\partial}{\partial t} |\Psi_{n_0}(t)\rangle = H |\Psi_{n_0}(t)\rangle; \quad (8)$$

here, H is given by Eq. (5), and $|\Psi_{n_0}(t)\rangle$ is sought in terms of the complete set of eigenstates based on the instantaneous eigenstates of H_0 and the eigenstates of H_r , subject to an initial Bloch momentum state and initial photon field occupancy. The instantaneous eigenstates of H_0 satisfy the equation¹⁵

$$\left(\frac{1}{2m_0} [\mathbf{p} + \mathbf{p}_c(t)]^2 + V_c(\mathbf{r}) \right) \psi_{n_0\mathbf{k}(t)} = \varepsilon_{n_0}[\mathbf{k}(t)] \psi_{n_0\mathbf{k}(t)}, \quad (9)$$

where

$$\psi_{n_0\mathbf{k}(t)}(\mathbf{r}, t) = \frac{e^{i\mathbf{K}\cdot\mathbf{r}}}{\Omega^{1/2}} u_{n_0\mathbf{k}(t)}(\mathbf{r}, t); \quad (10)$$

here, $u_{n_0\mathbf{k}(t)}(\mathbf{r}, t)$ is the periodic part of the Bloch function, $\mathbf{k}(t) = \mathbf{K} + (1/\hbar) \int_{t_0}^t \mathbf{F}(t') dt' = \mathbf{K} + \mathbf{p}_c(t)/\hbar$, where the values of

\mathbf{K} are determined by the periodic boundary conditions of the periodic crystal of volume Ω . The basis states for H_r are given by the well-known free photon field equation,

$$H_r|\{n_{\mathbf{q},j}\}\rangle = \sum_{\mathbf{q},j} \hbar\omega_{\mathbf{q},j}n_{\mathbf{q},j}|\{n_{\mathbf{q},j}\}\rangle, \quad (11)$$

where $|\{n_{\mathbf{q},j}\}\rangle$ is a simple product of all possible combinations of photon number states, $n_{\mathbf{q},j}$, with a given wave vector \mathbf{q} and polarization $\hat{\epsilon}_{\mathbf{q},j}$.

Thus, the solution to $|\Psi_{n_0}(t)\rangle$ of Eq. (8) can be represented in terms of eigenstates of basis states $|\psi_{n_0\mathbf{k}(t)},\{n_{\mathbf{q},j}\}\rangle = |\psi_{n_0\mathbf{k}(t)}\rangle|\{n_{\mathbf{q},j}\}\rangle$ of the unperturbed Hamiltonian H_0+H_r as

$$|\Psi_{n_0}(t)\rangle = \sum_{\mathbf{k}} \sum_{\{n_{\mathbf{q},j}\}} A_{\{n_{\mathbf{q},j}\}}(\mathbf{k},t) |\psi_{n_0\mathbf{k}(t)},\{n_{\mathbf{q},j}\}\rangle \times \exp\left(-\frac{i}{\hbar} \int_{t_0}^t [\varepsilon_{n_0}[\mathbf{k}(t')] + \sum_{\mathbf{q},j} \hbar\omega_{\mathbf{q},j}n_{\mathbf{q},j}] dt'\right), \quad (12)$$

where the summation over \mathbf{k} is carried out over the entire Brillouin zone (BZ), and $\{n_{\mathbf{q},j}\}$ is specified over all possible combinations of photon occupation number with corresponding photon wave vectors \mathbf{q} and polarization $\hat{\epsilon}_{\mathbf{q},j}$.

The appropriate time-dependent equations of motion for the $A_{\{n_{\mathbf{q},j}\}}(\mathbf{k},t)$ coefficients expressed in Eq. (12) are given in Appendix A; these equations relate the time dependence of $A_{\{n_{\mathbf{q},j}\}}(\mathbf{k},t)$ to the basis-dependent matrix elements of H_I through a self-consistent set of equations. In applying the usual first-order time-dependent perturbation theory methodology to this set of equations, consistent with the initial conditions for the \mathbf{k} state of the Bloch electron in the energy band “ n_0 ” and the initial state of radiation field, a first-order perturbation theory result, namely, $A_{\{n_{\mathbf{q},j}\}}^{(1)}(\mathbf{k},t) = A_{\{n_{\mathbf{q},j}\}}^{(a)}(\mathbf{k},t) + A_{\{n_{\mathbf{q},j}\}}^{(e)}(\mathbf{k},t)$, is obtained, where the superscripts “ a ” and “ e ” stand for photon absorption and emission, respectively. The explicit expressions for both $A_{\{n_{\mathbf{q},j}\}}^{(a)}(\mathbf{k},t)$ and $A_{\{n_{\mathbf{q},j}\}}^{(e)}(\mathbf{k},t)$ are given in Appendix A, in Eqs. (A6) and (A7).

In the case of photon emission, the total emission probability can be written as

$$P_e(t) = \sum_{\mathbf{q},j} (n_{\mathbf{q},j}^0 + 1) |A_{\mathbf{q},j}^{(e)}(\mathbf{k}_0,t)|^2, \quad (13)$$

where

$$A_{\mathbf{q},j}^{(e)}(\mathbf{k}_0,t) = \frac{D}{\sqrt{q}} \int_{t_0}^t dt' \mathbf{v}[\mathbf{k}_0(t') - \mathbf{q}] \cdot \hat{\epsilon}_{\mathbf{q},j} \times \exp\left(-\frac{i}{\hbar} \int_{t_0}^{t'} [\varepsilon_{n_0}[\mathbf{k}_0(t_1)] - \varepsilon_{n_0}[\mathbf{k}_0(t_1) - \mathbf{q}] - \hbar\omega_{\mathbf{q},j}] dt_1\right), \quad (14)$$

with $\mathbf{k}_0(t) = \mathbf{K}_0 + \mathbf{p}_c(t)/\hbar$. Here, \mathbf{K}_0 and $n_{\mathbf{q},j}^0$ are the initial values of the wave vector \mathbf{K} and photon number $n_{\mathbf{q},j}$, and $D = -i\sqrt{2\pi\alpha}/V$, where $\alpha = e^2/(\hbar c)$ is the fine structure constant.

It is clear from above that $|A_{\mathbf{q},j}^{(e)}[\mathbf{k}_0(t),t]|^2$ is the probability for the emission of a photon with wave vector \mathbf{q} and polarization $\hat{\epsilon}_{\mathbf{q},j}$ at time t . Yet, the total emission probability as calculated in first-order perturbation theory results in a weighted sum with respect to $(n_{\mathbf{q},j}^0 + 1)$ when summed over all photon wave number \mathbf{q} and polarization, as noted in Eq. (13). Therefore, it follows that if no photons are initially present in the quantum radiation field, that is $n_{\mathbf{q},j}^0 = 0$ for all modes, then the emission process results in the well-known SE probability,

$$P_e^s(t) = \sum_{\mathbf{q},j} |A_{\mathbf{q},j}^{(e)}(\mathbf{k}_0,t)|^2. \quad (15)$$

The additional term, proportional to $n_{\mathbf{q},j}^0$, in Eq. (13) is also well known to correspond to induced emission probability.

The terms associated with photon absorption in Eq. (A6) can be considered in a similar way; here we find, for the absorption probability, that

$$P_a(t) = \sum_{\mathbf{q},j} n_{\mathbf{q},j}^0 |A_{\mathbf{q},j}^{(a)}(\mathbf{k}_0,t)|^2, \quad (16)$$

where

$$A_{\mathbf{q},j}^{(a)}(\mathbf{k}_0,t) = \frac{D}{\sqrt{q}} \int_{t_0}^t dt' \mathbf{v}[\mathbf{k}_0(t') + \mathbf{q}] \cdot \hat{\epsilon}_{\mathbf{q},j} \times \exp\left(-\frac{i}{\hbar} \int_{t_0}^{t'} [\varepsilon_{n_0}[\mathbf{k}_0(t_1)] - \varepsilon_{n_0}[\mathbf{k}_0(t_1) + \mathbf{q}] + \hbar\omega_{\mathbf{q},j}] dt_1\right). \quad (17)$$

The quantity $P_a(t)$ in Eq. (16) is proportional to $n_{\mathbf{q},j}^0$ and therefore vanishes if the radiation field is initially in the vacuum state.

B. Properties of transition probabilities and selection rules for spontaneous emission of a single photon

The specific analysis now focuses on one-photon spontaneous emission from a Bloch band “ n_0 ” coupled to a radiation field that initially has no photons present. This means that the probability amplitude in the wave function of Eq. (12) satisfies the initial condition $A_{\{n_{\mathbf{q},j}\}}(\mathbf{k},t_0) = \{\delta_{n_{\mathbf{q},j},0}\} \delta_{\mathbf{K},\mathbf{K}_0}$ at time $t=t_0$ when the electric field is turned on. With this assumed initial condition, the probability amplitude for emission, $A_{\mathbf{q},j}^{(e)}(\mathbf{k}_0,t)$, is now evaluated from Eq. (14).

In evaluating $A_{\mathbf{q},j}^{(e)}(\mathbf{k}_0,t)$, it is assumed that the external dc field, \mathbf{E} , is along the z axis (also the growth direction of a SL); then, it follows that $k_{0z}(t) = K_{0z} + F(t-t_0)/\hbar$, and $\mathbf{k}_{0\perp}(t) = \mathbf{K}_{0\perp} = \text{const}$, where $\mathbf{k}_{0\perp}(t)$ is the component of wave vector $\mathbf{k}_0(t)$ perpendicular to the z axis. In taking advantage of the periodic properties of the terms in Eq. (14), $A_{\mathbf{q},j}^{(e)}(\mathbf{k}_0,t)$ is evaluated in *clocked* integral multiples of the Bloch period, so that $t = N\tau_B$, where $\tau_B = 2\pi/\omega_B$, the time to traverse one period of the BZ. Then, the integral in Eq. (14) over time can be replaced by an integral over k_{0z} through the substitution $dt = (\hbar/F) dk_{0z}$. It then follows from the periodic property of

the energy band in the BZ, and therefore the electron velocity as well, that the probability amplitude, at integral multiples of the Bloch period, can be expressed as¹⁵

$$A_{\mathbf{q},j}^{(e)}(\mathbf{k}_0, N\tau_B) = \left(\frac{1 - \exp(-iN\beta_q)}{1 - \exp(-i\beta_q)} \right) A_{\mathbf{q},j}^{(e)}(\mathbf{k}_0, \tau_B). \quad (18)$$

Here, the parameter β_q is given by

$$\beta_q = \frac{1}{F} \int_{K_{0z}}^{K_{0z}+G_z} [\varepsilon_{n_0}(\mathbf{k}_0) - \varepsilon_{n_0}(\mathbf{k}_0 - \mathbf{q}) - \hbar\omega_q] dk_{0z}, \quad (19)$$

and $A_{\mathbf{q},j}^{(e)}(\mathbf{k}_0, \tau_B)$, the probability amplitude over a single Bloch period, is

$$\begin{aligned} A_{\mathbf{q},j}^{(e)}(\mathbf{k}_0, \tau_B) &= \frac{\hbar D}{F\sqrt{q}} \int_{K_{0z}}^{K_{0z}+G_z} dk_{0z} \mathbf{v}(\mathbf{k}_0 - \mathbf{q}) \cdot \hat{\varepsilon}_{\mathbf{q},j} \\ &\times \exp\left(-\frac{i}{F} \int_{K_{0z}}^{k_{0z}} [\varepsilon_{n_0}(\mathbf{k}'_0) - \varepsilon_{n_0}(\mathbf{k}'_0 - \mathbf{q}) - \hbar\omega_q] dk'_{0z}\right), \end{aligned} \quad (20)$$

where $G_z = 2\pi/a$, the z component of the SL reciprocal-lattice vector. It then follows from Eq. (18) that

$$|A_{\mathbf{q},j}^{(e)}(\mathbf{k}_0, N\tau_B)|^2 = \frac{\sin^2(N\beta_q/2)}{\sin^2(\beta_q/2)} |A_{\mathbf{q},j}^{(e)}(\mathbf{k}_0, \tau_B)|^2. \quad (21)$$

From Eq. (21), it is seen that $|A_{\mathbf{q},j}^{(e)}(\mathbf{k}_0, N\tau_B)|^2$ will reach its maximum growth value when $\beta_q = 2\pi(m + \delta)$, where m is an integer and $\delta \rightarrow 0$; for this limit, the function $\sin^2(N\beta_q/2)/\sin^2(\beta_q/2) \rightarrow N^2$. It is clear that this condition for maximum growth establishes the *selection rule*¹⁵ for the photon emission frequency. Indeed, from the condition $\beta_q = 2\pi m$, it follows from Eq. (19) that

$$\omega_q = m\omega_B + \frac{1}{\hbar G_z} \int_{K_{0z}}^{K_{0z}+G_z} [\varepsilon_{n_0}(\mathbf{k}_0) - \varepsilon_{n_0}(\mathbf{k}_0 - \mathbf{q})] dk_{0z}. \quad (22)$$

In noting the contribution from the integral in Eq. (22), note that if \mathbf{q} is collinear with the direction of the applied field, i.e., in the z direction, then the integral in Eq. (22) vanishes because of the periodicity of $\varepsilon_{n_0}(\mathbf{k}_0)$. If, however, \mathbf{q} is not collinear with the direction of the applied field, then the integral in Eq. (22) does not vanish, and contributes to the selection rule. In particular, in considering the radiative long-wavelength limit, where $\varepsilon_{n_0}(\mathbf{k}_0 - \mathbf{q})$ can be expanded in a Taylor series about small q , the expression for ω_q in Eq. (22) results in

$$\omega_q = m\omega_B + \mathbf{q}_\perp \cdot \bar{\mathbf{v}}_\perp(\mathbf{K}_\perp). \quad (23)$$

Here, \mathbf{q}_\perp is the perpendicular component of \mathbf{q} relative to the applied electric field direction and the average transverse velocity, $\bar{\mathbf{v}}_\perp$, is given by

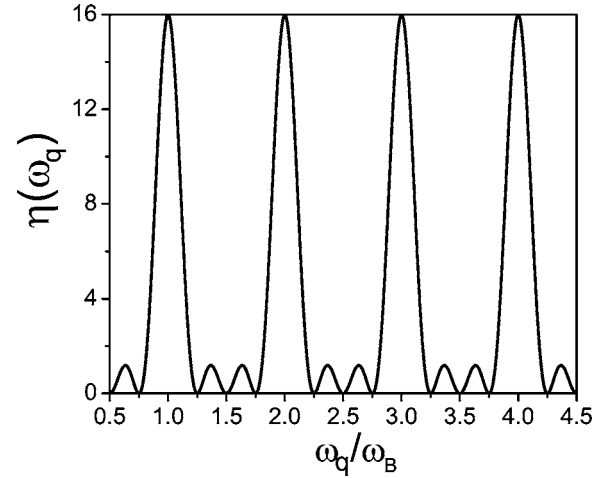


FIG. 1. Dependence of the relative probability spectral density $\eta(\omega_q)$ of SE on the normalized photon frequency ω_q/ω_B .

$$\bar{\mathbf{v}}_\perp(\mathbf{K}_\perp) = (1/G_z) \int_{K_{0z}}^{K_{0z}+G_z} \mathbf{v}_\perp(\mathbf{k}_0) dk_{0z}, \quad (24)$$

with $\mathbf{v}_\perp(\mathbf{k}_0) = (1/\hbar)\nabla_{\mathbf{K}_\perp}\varepsilon_{n_0}(\mathbf{K})|_{\mathbf{k}_0}$. Specifically for the tight-binding energy band approximation,¹⁸ one finds that $\bar{\mathbf{v}}_\perp(\mathbf{K}_\perp) = \mathbf{v}_\perp(\mathbf{K}_\perp)$. However, the second term on the right-hand side of Eq. (23) is negligibly small for nonrelativistic Bloch electron velocities;¹⁹ thus one generally has

$$\omega_q \approx m\omega_B, \quad q \approx q_m = m\frac{\omega_B}{c}, \quad (25)$$

the “Stark ladder” resonance condition.¹⁵

Figure 1 illustrates the resonance frequency behavior of the relative probability spectral density $\eta(\omega_q) = |A_{\mathbf{q},j}^{(e)}(\mathbf{k}_0, N\tau_B)|^2 / |A_{\mathbf{q},j}^{(e)}(\mathbf{k}_0, \tau_B)|^2$ for $N=4$. With increasing N , the $\eta(\omega_q)$ becomes sharply peaked at the resonances because the function $y(x) = \sin^2(N\pi x) / [N \sin^2(\pi x)]$ behaves like a delta function at each N as $x \rightarrow 0$. Thus, the modes that radiate with the highest probability correspond to the fundamental Bloch frequency and its harmonics; this quantization condition is obtained without requiring any assumptions concerning the existence of Wannier-Stark energy states.

C. Total spontaneous emission probability

The total SE probability is evaluated from Eq. (15). The SE probability is evaluated at time $t = N\tau_B$ by substituting $|A_{\mathbf{q},j}^{(e)}(\mathbf{k}_0, N\tau_B)|^2$, already obtained in Eq. (21), into Eq. (15) to obtain

$$\begin{aligned} P_e^s &\equiv P_e^s(N\tau_B) \\ &= \frac{V}{(2\pi)^3} \int_0^{q_{\max}} dq q^2 \frac{\sin^2(N\beta_q/2)}{\sin^2(\beta_q/2)} \int_0^{4\pi} d\Omega \sum_j |A_{\mathbf{q},j}^{(e)}(\mathbf{k}_0, \tau_B)|^2. \end{aligned} \quad (26)$$

Here, the sum over \mathbf{q} in Eq. (15) has been replaced by an integral over \mathbf{q} for a single polarization, such that $\sum_{\mathbf{q}}(\dots) \rightarrow [V/(2\pi)^3] \int dq q^2 \int d\Omega(\dots)$, where $d\Omega = \sin\theta d\theta d\varphi$ is the

element of a solid angle subtended by \mathbf{q} , and θ, φ are the polar angles. In treating the integral of Eq. (26), it is observed in the integral that $q^2 \sum_j |A_{\mathbf{q},j}^{(e)}(\mathbf{k}_0, \tau_B)|^2$ is a slowly varying function of q ; whereas, it is noted from Fig. 1, and previous discussions therein, that the term $\sin^2(N\beta_q/2)/\sin^2(\beta_q/2)$ is a sharply peaked, symmetric function of q at q values of $q_m = m\omega_B/c$, where m is an integer, as noted in Eq. (25). Thus, at every node defined by the resonance conditions $\beta_q = 2\pi m$, with $\omega_q/\omega_B = m$ and $q_m = m\omega_B/c$, the slowly varying function of q in the integrand can be replaced by its value evaluated at $q = q_m$, and then removed from the integral over q ; the remaining term in the integrand can be evaluated by letting $q = (\omega_B/2\pi c)\beta_q$ at each node so that

$$\int dq \frac{\sin^2(N\beta_q/2)}{\sin^2(\beta_q/2)} = \frac{\omega_B}{\pi c} \int_{-\pi}^{\pi} \frac{d\beta_q \sin^2(N\beta_q/2)}{2 \sin^2(\beta_q/2)} = N \frac{\omega_B}{c}.$$

Thus, Eq. (26) becomes

$$P_e^s = N \frac{\omega_B}{c} \frac{V}{(2\pi)^3} \sum_{l=1}^{l_{\max}} q_l^2 \int_0^{4\pi} d\Omega \sum_j |A_{\mathbf{q},j}^{(e)}(\mathbf{k}_0, \tau_B)|^2, \quad (27)$$

where l_{\max} follows from $q_{\max} = l_{\max} \omega_B/c$, and determines the upper limit in the sum over higher Bloch oscillation harmonics.

The calculation of P_e^s in Eq. (27) now requires the use of $A_{\mathbf{q},j}^{(e)}(\mathbf{k}_0, \tau_B)$ in Eq. (20), evaluated at the maximum growth conditions of Eq. (23), that is when $\hbar\omega_q = m\hbar\omega_B + \hbar\mathbf{q}_{\perp} \cdot \bar{\mathbf{v}}_{\perp}(\mathbf{K}_{\perp})$. In addition, the dependence upon \mathbf{q} in Eq. (20) is made explicit by invoking the assumption of a photon long-wavelength limit; this assumption is valid for all periodic potentials of interest, even SLs, where $q \ll \pi/a$. Thus, in letting $\varepsilon_{n_0}(\mathbf{k}_0 - \mathbf{q}) \approx \varepsilon_{n_0}(\mathbf{k}_0) - \mathbf{q} \cdot \nabla_{\mathbf{k}_0} \varepsilon_{n_0}(\mathbf{k}_0)$ and $\mathbf{v}(\mathbf{k}_0 - \mathbf{q}) \approx \mathbf{v}(\mathbf{k}_0) - \mathbf{q} \cdot \nabla_{\mathbf{k}_0} \mathbf{v}(\mathbf{k}_0)$, $A_{\mathbf{q},j}^{(e)}(\mathbf{k}_0, \tau_B)$ in Eq. (20) becomes, in the long-wavelength limit,

$$\begin{aligned} A_{\mathbf{q},j}^{(e)}(\mathbf{k}_0, \tau_B) &= \frac{\hbar D}{F\sqrt{q}} e^{i\varphi(K_{0z})} \int_{K_{0z}}^{K_{0z}+G_z} dk_{0z} \mathbf{v}(\mathbf{k}_0) \cdot \hat{\varepsilon}_{\mathbf{q},j} e^{-i[\varphi(k_{0z}) + \chi(k_{0z}, K_{0z})]}, \end{aligned} \quad (28)$$

with the phase factors in the exponent defined by

$$\varphi(x) = a \left(mx - q_z \frac{\varepsilon_{n_0}(x)}{\hbar\omega_B} \right), \quad (29a)$$

$$\chi(k_{0z}, K_{0z}) = \frac{a}{\omega_B} \left((k_{0z} - K_{0z}) \mathbf{q}_{\perp} \cdot \bar{\mathbf{v}}_{\perp} - \int_{K_{0z}}^{k_{0z}} dk'_{0z} \mathbf{q}_{\perp} \cdot \mathbf{v}_{\perp} \right). \quad (29b)$$

The results of Eqs. (28) and (29) are valid for an arbitrary band structure. But for the tight-binding band structure model cases now considered, especially since they are appropriate for SLs, it is noted that¹⁸ $\bar{\mathbf{v}}_{\perp} = \mathbf{v}_{\perp}$ in Eqs. (29b), in which case $\chi(k_{0z}, K_{0z}) \equiv 0$. Therefore, for the tight-binding model, Eq. (28) can be simplified by introducing dimensionless variables and parameters,

$$\vartheta_k = k_{0z}a, \quad \vartheta_q = q_z a, \quad \varepsilon_B(\vartheta_k) = \frac{\varepsilon_{n_0}(k_{0z})}{\hbar\omega_B}. \quad (30)$$

Then the integral in Eq. (28) becomes

$$A_{\mathbf{q},j}^{(e)}(\mathbf{k}_0, \tau_B) = - \frac{2\pi D}{\omega_B \sqrt{q}} e^{i\varphi(K_{0z})} \Phi_{mj}(\vartheta_q), \quad (31)$$

where

$$\Phi_{mj}(\vartheta_q) = \frac{1}{2\pi} \int_{-\pi}^{\pi} d\vartheta_k \Gamma_{\mathbf{q},j}(\vartheta_k) e^{-im\vartheta_k}, \quad (32)$$

the m th Fourier component of the integrand $\Gamma_{\mathbf{q},j}(\vartheta_k) = \mathbf{v} \cdot \hat{\varepsilon}_{\mathbf{q},j} e^{i\vartheta_q \varepsilon_B(\vartheta_k)}$. Thus, it follows from Eq. (31) that

$$|A_{\mathbf{q},j}^{(e)}(\mathbf{k}_0, \tau_B)|^2 = \frac{4\pi^2 |D|^2}{\omega_B^2 q} |\Phi_{mj}(\vartheta_q)|^2, \quad (33)$$

where D is defined after Eq. (14). Substituting Eq. (33) into Eq. (27), one obtains

$$P_e^s = \frac{\alpha N}{\omega_B c} \sum_{l=1}^{l_{\max}} q_l \int_0^{4\pi} d\Omega \sum_j |\Phi_{lj}(\vartheta_{q_l})|^2. \quad (34)$$

In analyzing the polarization properties of the SE, it is convenient to separate the contribution to $\Phi_{mj}(\vartheta_q)$ with polarization parallel and perpendicular to the applied electric field, i.e., relative to the z axis, so that $\Phi_{mj}(\vartheta_q) = \Phi_{mj,z}(\vartheta_q) + \Phi_{mj,\perp}(\vartheta_q)$, where

$$\Phi_{mj,z}(\vartheta_q) = (\hat{\varepsilon}_{\mathbf{q},j})_z \frac{1}{2\pi} \int_{-\pi}^{\pi} d\vartheta_k v_z(\vartheta_k) e^{i[\vartheta_q \varepsilon_B(\vartheta_k) - m\vartheta_k]} \quad (35)$$

and

$$\Phi_{mj,\perp}(\vartheta_q) = (\hat{\varepsilon}_{\mathbf{q},j})_{\perp} \cdot \frac{1}{2\pi} \int_{-\pi}^{\pi} d\vartheta_k \mathbf{v}_{\perp}(\vartheta_k) e^{i[\vartheta_q \varepsilon_B(\vartheta_k) - m\vartheta_k]}. \quad (36)$$

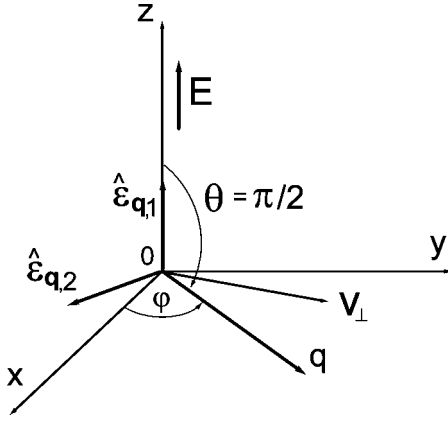
Here the symbol \perp stands for the vector component perpendicular to the applied electric field. These terms determine angular dependences of the intensity of SE. The next step is to evaluate the integrals in Eqs. (35) and (36), which requires a specific model for the energy band structure. This will be addressed in the next section.

IV. ANALYSIS OF SPONTANEOUS EMISSION FOR SUPERLATTICE AND TIGHT-BINDING MODELS

The analysis for spontaneous emission and radiation characteristics is now developed by utilizing the special case of a SL miniband with a growth direction defined along the z axis. The electron energy band dispersion relation is expressed as

$$\varepsilon_{n_0}(\mathbf{K}) = \varepsilon_{n_0}(0) + \sum_{l=1}^{\infty} \Delta_l \sin^2 \frac{K_z l a}{2} + \Delta \varepsilon(\mathbf{K}_{\perp}), \quad (37)$$

where $\varepsilon_{n_0}(0)$ is the band edge, Δ_l is the width of the l th miniband harmonic of the SL, and $\Delta \varepsilon(\mathbf{K}_{\perp})$ is the contribu-

FIG. 2. Geometry of radiation for transverse SE ($\theta = \pi/2$).

tion from the perpendicular components of the band. The corresponding velocity, for the given K_z in the z direction, is then given by $v_z(K_z) = (1/\hbar)[\partial \varepsilon_{n_0}(K_z)/\partial K_z] = \sum_{l=1}^{\infty} v_l \sin(K_z l a)$, where $v_l = \Delta_l l a / 2\hbar$, the maximum velocity associated with the l th miniband of bandwidth, Δ_l . The energy band dispersion of Eq. (37) in the SL direction generally includes long range coupling over the neighboring QWs with a relative strength measured by the specific value of the ratio $\Delta_{l+1}/\Delta_l < 1$, which is dependent upon the extent of wave function overlap. For the well-known case of nearest-neighbor tight-binding (NNTB) energy dispersion, only Δ_1 is considered significant, so that next nearest neighbor and longer range QW wave function overlaps are assumed to be negligibly small. Also for the energy band model under consideration in Eq. (37), it is noted that $\mathbf{v}_{\perp}(\mathbf{k}_0)$ is independent of k_{0z} , so that $\bar{\mathbf{v}}_{\perp} = \mathbf{v}_{\perp}$ (Ref. 18) from Eq. (24), and for subsequent use in Eq. (36).

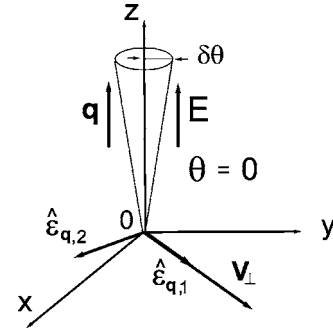
A. Direction of spontaneous emission radiation output relative to the electric field

First, it is useful to analyze the particular cases of SE probability for the \mathbf{q} direction of propagation, where \mathbf{q} is perpendicular to \mathbf{E} , the transverse radiation direction, and then where \mathbf{q} is parallel to \mathbf{E} , the longitudinal radiation direction. Finally, this will be followed by the case where \mathbf{q} is at an arbitrary direction with respect to the electric field.

1. Radiation in transverse direction

For the case of the photon wave vector, \mathbf{q} , perpendicular to the applied field, \mathbf{E} , then as noted from Fig. 2, $q_z = 0$ and $q = |\mathbf{q}_{\perp}|$; also, the two independent polarization directions, $\hat{\varepsilon}_{\mathbf{q},j}$, can be chosen parallel to the field direction, with longitudinal polarization [referred to as L polarization, with $j=1$ and $(\hat{\varepsilon}_{\mathbf{q},1})_z = 1$, $(\hat{\varepsilon}_{\mathbf{q},1})_{\perp} = 0$], and perpendicular to the field direction, with transverse polarization [referred to as T polarization, with $j=2$ and $(\hat{\varepsilon}_{\mathbf{q},2})_z = 0$, $|(\hat{\varepsilon}_{\mathbf{q},2})_{\perp}| = 1$]. Since $q_z = 0$, it follows from Eq. (30) that $\vartheta_q = 0$ so that Eqs. (35) and (36) become analytically manageable for evaluation, and one obtains

$$\Phi_{mj,z}(0) = -\frac{i}{2}(\hat{\varepsilon}_{\mathbf{q},j})_z \sum_{l=1}^{\infty} v_l \delta_{l,m} = -\frac{i}{2}(\hat{\varepsilon}_{\mathbf{q},j})_z v_m,$$

FIG. 3. Geometry of radiation for longitudinal SE ($\theta = 0$).

$$\Phi_{mj,\perp}(0) = (\mathbf{v} \cdot \hat{\varepsilon}_{\mathbf{q},j})_{\perp} \delta_{m,0}. \quad (38)$$

Thus, for L polarization, only the $l=m$ term survives, which is in resonance with the m th Bloch harmonic oscillation. In contrast, the model with NNTB, which is frequently used to approximate electron transport in narrow energy bands, would allow the generation of $l=1$ only, thereby limiting the propagation to the fundamental Bloch harmonic.

Substituting $\Phi_{mj,z}(0)$ from Eq. (38) into Eq. (33), the L polarization probability amplitude becomes

$$|A_{\mathbf{q},1}^{(e)}(\mathbf{k}_0, \tau_B)|^2 = \alpha \frac{2\pi^3}{V} \frac{1}{q} \frac{v_m^2}{\omega_B^2} R_T(\varphi), \quad (39)$$

where $R_T(\varphi)$ is introduced as an angular form factor. The emission probability density is independent of the angle φ , the angle the \mathbf{q} makes with the x axis in the xy plane (see Fig. 2). Thus, the form factor $R_T(\varphi)$, denoted by $R_T(\theta = \pi/2, \varphi)$ is unity on the right-hand side of Eq. (39). Thus, the SE probability is

$$P_e^s = \frac{\alpha N}{4\omega_B c} \sum_{l=1}^{l_{\max}} q_l v_l^2 \delta\Omega = \frac{\alpha}{4} N \sum_{l=1}^{l_{\max}} l \frac{v_l^2}{c^2} \delta\Omega, \quad (40)$$

where account has been taken for photon wave vector $q_l = l\omega_B/c$ and the small solid angle $\delta\Omega = 2\pi \delta\theta$ for $\theta \in [(\pi - \delta\theta)/2, (\pi + \delta\theta)/2]$, $\delta\theta \ll 1$.

The emission of photons with T polarization gives a zero contribution into P_e^s , since the condition ($m=l=0, j=2$) in Eq. (38) results in zero wave vector $q_{l=0}=0$.

2. Radiation in longitudinal direction

For the case of the photon wave vector, \mathbf{q} , parallel to the applied field, \mathbf{E} , while the polarization $\hat{\varepsilon}_{\mathbf{q},j}$ is perpendicular to the direction of the field, then consider $q = |q_{\perp}|$, $\mathbf{q}_{\perp} = 0$ with $(\hat{\varepsilon}_{\mathbf{q},j})_z = 0$ and $|(\hat{\varepsilon}_{\mathbf{q},j})_{\perp}| = 1$. The two independent polarizations, $\hat{\varepsilon}_{\mathbf{q},j}$, are chosen, as noted in Fig. 3. In this case, since $\vartheta_q \neq 0$, the term $\Phi_{mj,\perp}(\vartheta_q)$ in Eq. (36) can be calculated analytically if we omit the higher harmonic contribution ($l > 1$) in the energy band dispersion of Eq. (37). Then Eq. (36) becomes

$$\Phi_{mj,\perp}(\vartheta_q) = (\mathbf{v} \cdot \hat{\varepsilon}_{\mathbf{q},j})_{\perp} J_m \left(\frac{\vartheta_q \Delta_l}{2\hbar \omega_B} \right) \exp(-i\pi m/2), \quad (41)$$

where $J_m(x)$ is the Bessel function of the first kind.

Thus, from Eq. (41) the longitudinal component of SE will be nonvanishing for finite values of \mathbf{v}_\perp ; the electron just moves along the in-plane direction at a constant \mathbf{v}_\perp , which is fixed by the initial quasimomentum. Substituting Eq. (41) into Eq. (33), the probability amplitude becomes

$$|A_{\mathbf{q},j}^{(e)}(\mathbf{k}_0, \tau_B)|^2 = \alpha \frac{(2\pi)^3}{V} \frac{1}{q} \frac{(\mathbf{v} \cdot \hat{\boldsymbol{\epsilon}}_{\mathbf{q},j})_\perp^2}{\omega_B^2} J_m^2\left(\frac{\partial_q \Delta_1}{2\hbar\omega_B}\right) R_L(\varphi). \quad (42)$$

Then, from Eq. (34), the SE probability becomes

$$P_e^s = \frac{\alpha N}{\omega_B c} \mathbf{v}_\perp^2 \sum_{l=1}^{l_{\max}} q_l J_l^2\left(\frac{\partial_q \Delta_1}{2\hbar\omega_B}\right) \delta\Omega, \quad (43)$$

where $\delta\Omega = 2\pi[1 - \cos(\delta\theta)] \approx \pi(\delta\theta)^2$, the small solid angle about the z axis, where $\delta\theta \ll 1$. The photon polarization perpendicular to the velocity \mathbf{v}_\perp does not contribute to the SE. $R_L(\varphi)$, the emission form factor in Eq. (42), is isotropic in the xy plane of Fig. 3; therefore $R_L(\varphi) = R_L(\theta=0, \varphi) = 1$. By utilizing the fact that $q_l = l\omega_B/c$ in the argument of the Bessel function in Eq. (43), it follows that $\partial_{q_l} \Delta_1 / (2\hbar\omega_B) = lv_1/c \ll 1$. Thus, the asymptotic form for $J_l(x) \approx (x/2)^l / \Gamma(l+1)$, for $x \ll 1$ is assumed, where $\Gamma(x)$ is the gamma function, and $v_1 = \Delta_1 a / 2\hbar$; therefore, P_e^s in Eq. (43) reduces to

$$P_e^s = \alpha N (\mathbf{v}_\perp / c)^2 \sum_{l=1}^{l_{\max}} \frac{l^{2l+1}}{4^l (l!)^2} \left(\frac{v_1}{c}\right)^{2l} \delta\Omega. \quad (44)$$

In particular, for the fundamental Bloch harmonic ($l=1$), Eq. (44) becomes

$$P_e^s = \frac{\alpha}{4} N \left(\frac{v_1}{c}\right)^2 (\mathbf{v}_\perp / c)^2 \delta\Omega. \quad (45)$$

3. Radiation in arbitrary direction

For the case of photon wave vector, \mathbf{q} , at an arbitrary angle with respect to the electric field, as noted in Fig. 4(a), the angular dependence of the SE probability can be elucidated from Eqs. (35) and (36). Since the integrals of Eqs. (35) and (36) can only be evaluated numerically when the full energy dispersion of Eq. (37) is used, use is made of the NNTB approximation in Eq. (37) by keeping the term with $l=1$ only in the dispersion relation. In this case, the longitudinal component, $\Phi_{mj,z}(\partial_q)$, in Eq. (35), is found to be, after integration

$$\Phi_{mj,z}(\partial_q) = (\hat{\boldsymbol{\epsilon}}_{\mathbf{q},j})_z \frac{m\omega_B}{q_z} J_m(v_1 q_z / \omega_B) \exp(-i\pi m/2). \quad (46)$$

In noting again, as in subsection IV A 2, that the argument of the Bessel function is small so that an asymptotic limit may be imposed, it follows that Eq. (46) reduces to $\Phi_{mj,z}(\partial_q) = (\hat{\boldsymbol{\epsilon}}_{\mathbf{q},j})_z v_1 m (v_1 q_z / \omega_B)^{m-1} \exp(-i\pi m/2) / (2^m m!)$.

The transverse component, $\Phi_{mj,\perp}(\partial_q)$, in Eq. (36) can be calculated in a similar fashion. It is found that

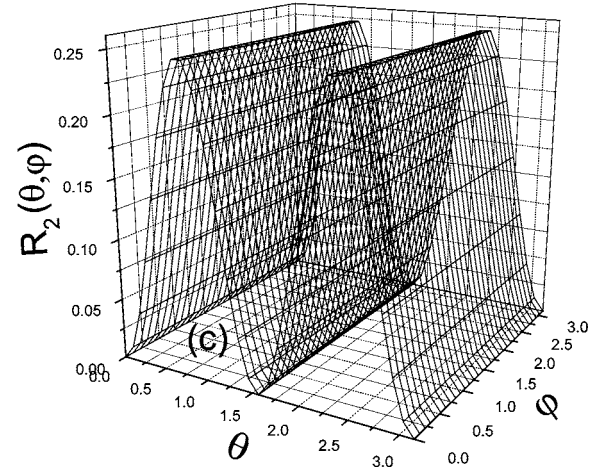
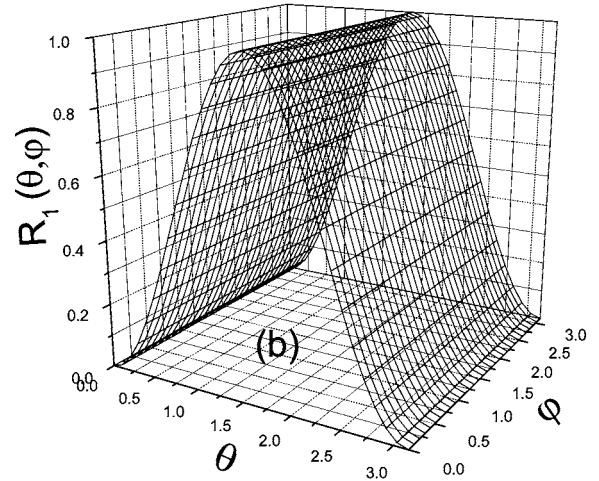
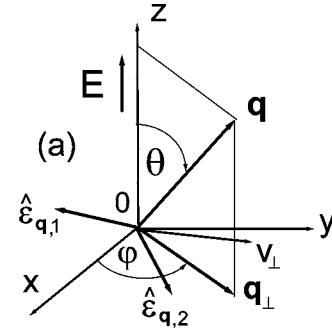


FIG. 4. (a) Geometry of radiation for an arbitrary wave vector \mathbf{q} . (b)–(c) Form factor $R_l(\theta, \varphi)$ of the SE probability; (b) fundamental Bloch frequency ($l=1$); (c) second Bloch harmonic ($l=2$).

$$|\Phi_{mj}(\partial_q)|^2 = \left((\hat{\boldsymbol{\epsilon}}_{\mathbf{q},j})_z m \frac{\omega_B}{q_z} + (\mathbf{v} \cdot \hat{\boldsymbol{\epsilon}}_{\mathbf{q},j})_\perp \right)^2 J_m^2(v_1 q_z / \omega_B). \quad (47)$$

For wave vectors \mathbf{q} with a z component projected over $q_z = q_{zm} \equiv (m\omega_B \cos \theta)/c$, the second term in the square bracket is small compared to the first term with respect to the parameter $\gamma = |\mathbf{v}_\perp|/c$, except in a narrow angular range defined by $\delta\theta \approx \gamma$. This correction can be taken into account through the

function $g_{m,j}(\theta, \varphi) = 1 + q_z(\mathbf{v} \cdot \hat{\mathbf{e}}_{\mathbf{q},j})_{\perp} / [m\omega_B(\hat{\mathbf{e}}_{\mathbf{q},j})_z]$, which is equal to 1 if the latter term is ignored. Then we obtain from Eqs. (34) and (47),

$$P_e^s = \alpha N \sum_{l=1}^{l_{\max}} l \int_0^{4\pi} \frac{d\Omega}{\cos^2 \theta} J_l^2 \left(l \frac{v_1}{c} \cos \theta \right) \sum_{j=1}^2 (\hat{\mathbf{e}}_{\mathbf{q},j})_z^2 g_{l,j}^2(\theta, \varphi). \quad (48)$$

For $v_1 l \sin \theta / c \ll 1$, this equation takes the form

$$P_e^s = \alpha N \sum_{l=1}^{l_{\max}} \frac{l^{2l+1}}{4^l (l!)^2} \left(\frac{v_1}{c} \right)^{2l} \int_0^{4\pi} d\Omega R_l(\theta, \varphi), \quad (49)$$

where the form factor

$$R_l(\theta, \varphi) = \cos^{2(l-1)}(\theta) \sum_{j=1}^2 (\hat{\mathbf{e}}_{\mathbf{q},j})_z^2 g_{l,j}^2(\theta, \varphi) \quad (50)$$

determines the angular dependence of the SE probability for the l th Bloch harmonic. In particular, at zero transverse velocity [$g_{l,j}(\theta, \varphi) = 1$], we obtain the form factor, taking into account the fundamental ($l=1$) and the second ($l=2$) Bloch frequency harmonics $R_1(\theta) = \sin^2(\theta)$ and $R_2(\theta) = (1/4)\sin^2(2\theta)$, respectively. For nonzero transverse velocity, the form factor depends on both polar angles (θ, φ), with the dependence on φ being weak according to the function $g_{l,j}(\theta, \varphi)$. Figures 4(b) and 4(c) illustrate the anisotropy of the form factor corresponding to the fundamental ($l=1$) and the second ($l=2$) Bloch harmonic. Finally, integrating over all polar angles, we find

$$P_e^s = \frac{2\pi}{3} \alpha N \left(\frac{v_1}{c} \right)^2 \left[1 + \frac{2}{5} \left(\frac{v_1}{c} \right)^2 \right]. \quad (51)$$

B. Spontaneous emission discussion; Power estimate

The spontaneous emission probability has been obtained and analyzed for a variety of directional outputs. In general, it is clear from Eq. (34) and (47) that the average probability per unit time, resulting from first-order time-dependent perturbation theory, is $P_e^s(t = N\tau_B) / (N\tau_B) \sim \omega_B$; in contrast, in a one-electron atom, with a two-level model, the resulting frequency dependence¹² for the rate of SE $\sim \omega_{eg}^3$, where ω_{eg} is the characteristic frequency corresponding to the electron transition between the excited state and the ground state. Thus, the SE probability of Bloch radiation has a comparatively weaker frequency dependence than the corresponding two-level atomic SE probability.

Finally, a numerical estimate is performed for purposes of evaluating the power generated during the spontaneous emission process. In this regard, a semiconductor SL of one micron length is considered, consisting of 100 periods with SL lattice parameter $a = 100 \text{ \AA}$, and with lateral cross section $S = 100 \times 100 \text{ \mu m}^2$. The SL is assumed to have an electron density of $5 \times 10^{17} \text{ cm}^{-3}$, which corresponds to a total number of electrons in the SL active region of $n = 5 \times 10^9$. For the SL miniband structure, in the NNTB approximation, it is assumed that the lowest miniband energy width, Δ_1 , is

20 meV, so that the maximum group velocity in the miniband [$l=1$; Eq. (37)] is $v_1 = a\Delta_1 / (2\hbar) = 1.6 \times 10^7 \text{ cm/s}$; these parameter magnitudes resemble those of GaAs-based SLs used to study high-frequency microwave generation.^{4,20,21}

Spontaneous emission is considered for a photon energy given by $\hbar\omega_q = \hbar\omega_B = 10 \text{ meV}$, which corresponds to the fundamental Bloch frequency $\nu_B = \omega_B / (2\pi) = 2.5 \text{ THz}$. The corresponding electric field required to achieve this Bloch frequency is $E = \hbar\omega_B / (ea) = 10 \text{ kV/cm}$, and results in the application of one volt across the SL. It then follows from Eq. (51) that the SE probability for $N=100$ is estimated²² to be $P_e^s(N=100) = 4.3 \times 10^{-7}$. From this SE probability, an estimate of the generation energy per electron becomes $\hbar\omega_B P_e^s = 4.3 \times 10^{-6} \text{ meV}$, and since there are a total of $n=5 \times 10^9$ electrons in the active region of the SL, the generated energy achievable is estimated to be $P = n\hbar\omega_B P_e^s = 21.7 \text{ eV}$, which corresponds to an approximate power generation of $W = (\nu_B / N)P \approx 0.1 \text{ \mu W}$. In this power estimate, it is noted that the power generated in W is proportional to ω_B^2 , and thus E^2 , as expected from power considerations. Although the power generated is discernibly low for SE of Bloch oscillation radiation into free space, it is noted that SE probabilities and rates can be modified by tailoring the surrounding resonant electromagnetic environment.¹²⁻¹⁴ It would therefore be interesting to consider the prospect of enhancing superlattice spontaneous emission of Bloch oscillation radiation through superlattice-resonant cavity interaction with the cavity tuned to the Bloch frequency, while, at the same time, admitting scattering processes as an offsetting suppressant; this is the subject of a future investigation.

V. SUMMARY AND DISCUSSION

A theory for the spontaneous emission of radiation for a Bloch electron traversing a single band in a uniform electric field and in a scattering-free environment has been developed. The analysis results in a selection rule that shows that spontaneous emission is sharply peaked at frequencies equal to integral multiples of the Bloch frequency, a result that made no *ad hoc* assumptions concerning the existence of Wannier-Stark quantized energy levels within the band, but that comes directly from the use of electric field-dependent instantaneous eigenstates of the Bloch Hamiltonian. Spontaneous emission probabilities were derived and analyzed in terms of band structure and polarization radiation properties. A theoretical estimate for the intensity of the spontaneous emission for GaAs-based superlattices resulted in a power output into free space of one-tenth of a microwatt.

The theoretical analysis has implicitly assumed a single electron model for a Bloch electron in a uniform electric field of a perfect superlattice crystal ignoring scattering effects. Such assumptions provide the optimal conditions for coherent Bloch oscillations and, therefore, reflect the conditions for the maximum achievable power output, albeit, one-tenth of a microwatt into free space, as calculated in Sec. IV. But in recent years, many studies on coherent Bloch oscillations have pointed to the importance of additional scattering effects such as carrier-carrier scattering,²⁵ LO-phonon scattering,²⁶ and alloy disorder (interface roughness) scattering²⁷

due to superlattice compositional doping, all effects that strongly influence the dephasing of coherent Bloch oscillations, and therefore have a significant influence on the magnitude of the spontaneous emission output. The dephasing effects result in a broadening of the peaks of the spontaneous emission probability function that determines the selection rule for transitions, in our case $\omega_q = m\omega_B$, and also dampen the output THz radiation amplitude. Specifically, interface roughness scattering²⁷ has been identified as a dominant mechanism for dephasing in GaAs/AlGaAs superlattices over a wide temperature range; competitive dephasing mechanisms have been reported due to LO-phonon emission in a miniband wider than the LO-phonon energy (36 meV for GaAs-based superlattices), and also from carrier-carrier scattering effects.^{25,26} In all cases, the estimated linewidth for broadening from such effects ranges as $\sim(1.25-2.5)$ meV, which corresponds to dephasing times in a range of $\sim(1.0-0.5)$ ps;²⁵⁻²⁷ this broadening in energy is nontrivial as it corresponds to about 20% of the Bloch frequency.

It is also noted that the external electric field in our analysis is assumed to be homogeneous across the active region of the superlattice. However, in a realistic device analysis, as the electron density is increased to achieve maximum efficiency for spontaneous emission, the Bloch oscillating superlattice can develop inhomogeneous fields. In this case, the developed theory can be extended by treating the Bloch electron dynamics in inhomogeneous electric fields of arbitrary strength and time dependence.^{15,28} In other situations, domain formation may be possible through negative differential conductance. In this case, by superlattice design, a superstructure can be tailored as a stack of superlattices of appropriate lengths to prevent domain formation.¹⁴

Last, it is noted that a Bloch oscillation superlattice does not require *controlled inversion population* between Wannier-Stark ladder levels to get the desired spontaneous emission photon frequency; the desired frequency is controlled by the applied field. Whereas in other superlattice light generating devices, such as quantum cascade lasers, a large inversion population is required to provide stimulated emission with resulting high threshold current densities and high heat dissipation. In this regard, the Bloch oscillator in spontaneous emission offers a novel option for operating at THz frequencies, provided the power output can be enhanced in the coherent Bloch regime.

In closing, the power emitted into free space from the spontaneous emission of Bloch oscillation radiation is discernibly small. It is our intention in a future effort to consider enhancing superlattice spontaneous emission of Bloch oscillation radiation through superlattice-cavity interaction with the cavity tuned to the Bloch frequency, while, at the same time, including the offsetting effects of dephasing inhomogeneities mentioned earlier, so as to more realistically evaluate the optimal magnitudes of power output from the spontaneous emission of Bloch oscillation radiation.

ACKNOWLEDGMENTS

This work was supported by the Office of Naval Research and the U.S. Army Research Office.

APPENDIX A: RESULTS OF PERTURBATION THEORY APPROACH

The equation for the probability amplitudes $A_{\{n_{q,j}\}}(\mathbf{k}, t)$ in Eq. (12) is given by

$$\begin{aligned} \frac{dA_{\{n_{q,j}\}}(\mathbf{k}, t)}{dt} = & \frac{1}{i\hbar} \sum_{\mathbf{k}'} \sum_{\{n'_{q,j}\}} A_{\{n'_{q,j}\}}(\mathbf{k}', t) \\ & \times \langle \{n_{q,j}\}, \psi_{n_0\mathbf{k}(t)} | H_I | \psi_{n_0\mathbf{k}'(t)}, \{n'_{q,j}\} \rangle \\ & \times \exp\left(-\frac{i}{\hbar} \int_{t_0}^t \left[\varepsilon_{n_0}[\mathbf{k}'(t')] - \varepsilon_{n_0}[\mathbf{k}(t')] \right. \right. \\ & \left. \left. + \sum_{q,j} (n'_{q,j} - n_{q,j}) \hbar \omega_q \right] dt'\right). \end{aligned} \quad (\text{A1})$$

We assume that at initial time, t_0 , the system is in one of the eigenstates of Hamiltonian $H_0 + H_r$ with wave function $|\psi_{n_0\mathbf{K}_0}, \{n_{q,j}^0\}\rangle$, corresponding to the Bloch electron in a single band “ n_0 ” with the wave vector \mathbf{K}_0 , i.e., $\psi_{n_0\mathbf{K}_0} = (1/\Omega^{1/2})e^{i\mathbf{K}_0\mathbf{r}}u_{n_0\mathbf{K}_0}$, and with the initial distribution of photon numbers in the radiation field $\{n_{q,j}^0\}$. Substituting $A_{\{n_{q,j}\}}(\mathbf{k}, t) = A_{\{n_{q,j}\}}^{(0)}(\mathbf{k}, t) + A_{\{n_{q,j}\}}^{(1)}(\mathbf{k}, t) + \dots$ into Eq. (A1), and taking into account the initial condition $A_{\{n_{q,j}\}}(\mathbf{k}, t_0) = \{\delta_{n_{q,j}, n_{q,j}^0}\} \delta_{\mathbf{k}(t), \mathbf{K}_0(t)}$, one obtains to the zeroth and first order in H_I , defined in Eq. (7), for $A_{\{n_{q,j}\}}^{(0)}(\mathbf{k}, t)$ and $A_{\{n_{q,j}\}}^{(1)}(\mathbf{k}, t)$, respectively,

$$A_{\{n_{q,j}\}}^{(0)}(\mathbf{k}, t) = \{\delta_{n_{q,j}, n_{q,j}^0}\} \delta_{\mathbf{k}(t), \mathbf{K}_0(t)}, \quad (\text{A2})$$

$$\begin{aligned} A_{\{n_{q,j}\}}^{(1)}(\mathbf{k}, t) = & \frac{1}{i\hbar} \int_{t_0}^t dt' \langle \{n_{q,j}\}, \psi_{n_0\mathbf{k}(t')} | H_I | \psi_{n_0\mathbf{k}_0(t')}, \{n_{q,j}^0\} \rangle \\ & \times \exp\left(-\frac{i}{\hbar} \int_{t_0}^{t'} \left[\varepsilon_{n_0}[\mathbf{k}_0(t'')] - \varepsilon_{n_0}[\mathbf{k}(t'')] \right. \right. \\ & \left. \left. + \sum_{q,j} (n_{q,j}^0 - n_{q,j}) \hbar \omega_q \right] dt''\right), \end{aligned} \quad (\text{A3})$$

where $\mathbf{k}_0(t) = \mathbf{K}_0 + \mathbf{p}_c(t)/\hbar$ and $\{\delta_{n_{q,j}, n_{q,j}^0}\} \equiv \prod_{q,j} \delta_{n_{q,j}, n_{q,j}^0}$. Matrix elements for perturbation operator H_I (Appendix B) are given by

$$\begin{aligned} & \langle \{n_{q,j}\}, \psi_{n_0\mathbf{k}(t)} | H_I | \psi_{n_0\mathbf{k}_0(t)}, \{n_{q,j}^0\} \rangle \\ & = \sqrt{\frac{2\pi\alpha}{V}} \sum_{\mathbf{q}', j'} \frac{\hat{\varepsilon}_{\mathbf{q}', j'}}{\sqrt{q'}} \nabla_{\mathbf{k}} \varepsilon_{n_0}[\mathbf{k}(t)] \\ & \times (\sqrt{n_{\mathbf{q}', j'}^0} (\delta_{n_{\mathbf{q}', j'}, n_{\mathbf{q}', j'}^0} \delta_{\mathbf{k}_0, \mathbf{k}-\mathbf{q}'}; \{\delta_{n_{q,j}, n_{q,j}^0}\}) \delta_{\mathbf{k}_0, \mathbf{k}-\mathbf{q}'} \\ & + \sqrt{n_{\mathbf{q}', j'}^0 + 1} (\delta_{n_{\mathbf{q}', j'}, n_{\mathbf{q}', j'}^0 + 1}; \{\delta_{n_{q,j}, n_{q,j}^0}\}) \delta_{\mathbf{k}_0, \mathbf{k}+\mathbf{q}'}, \end{aligned} \quad (\text{A4})$$

where $\alpha = e^2/(\hbar c)$ is the fine structure constant. Thus, we obtain

$$A_{\{n_{\mathbf{q},j}\}}^{(1)}(\mathbf{k}, t) = A_{\{n_{\mathbf{q},j}\}}^{(a)}(\mathbf{k}, t) + A_{\{n_{\mathbf{q},j}\}}^{(e)}(\mathbf{k}, t), \quad (\text{A5})$$

where the first term on the right-hand side of Eq. (A5) is due to absorption of a photon from the radiation field by the Bloch electron

$$\begin{aligned} A_{\{n_{\mathbf{q},j}\}}^{(a)}(\mathbf{k}, t) = & D \sum_{\mathbf{q}', j'} \sqrt{n_{\mathbf{q}', j'}^0} (\delta_{n_{\mathbf{q}', j'}, n_{\mathbf{q}', j'}^0 - 1}; \{\delta_{n_{\mathbf{q}, j}, n_{\mathbf{q}, j}^0}\}) \\ & \times \delta_{\mathbf{k}_0, \mathbf{k} + \mathbf{q}'} \frac{\hat{\mathbf{e}}_{\mathbf{q}', j'}}{\sqrt{q'}} \int_{t_0}^t dt' \mathbf{v}[\mathbf{k}(t')] \\ & \times \exp\left(-\frac{i}{\hbar} \int_{t_0}^{t'} [\varepsilon_{n_0}[\mathbf{k}_0(t'')] \right. \\ & \left. - \varepsilon_{n_0}[\mathbf{k}(t'')] + \hbar \omega_{q'}] dt''\right), \end{aligned} \quad (\text{A6})$$

and the second term represents emission of a photon by the Bloch electron to the radiation field

$$\begin{aligned} A_{\{n_{\mathbf{q},j}\}}^{(e)}(\mathbf{k}, t) = & D \sum_{\mathbf{q}', j'} \sqrt{n_{\mathbf{q}', j'}^0 + 1} (\delta_{n_{\mathbf{q}', j'}, n_{\mathbf{q}', j'}^0 + 1}; \{\delta_{n_{\mathbf{q}, j}, n_{\mathbf{q}, j}^0}\}) \\ & \times \delta_{\mathbf{k}_0, \mathbf{k} + \mathbf{q}'} \frac{\hat{\mathbf{e}}_{\mathbf{q}', j'}}{\sqrt{q'}} \int_{t_0}^t dt' \mathbf{v}[\mathbf{k}(t')] \\ & \times \exp\left(-\frac{i}{\hbar} \int_{t_0}^{t'} \{\varepsilon_{n_0}[\mathbf{k}_0(t'')] \right. \\ & \left. - \varepsilon_{n_0}[\mathbf{k}(t'')] - \hbar \omega_{q'}\} dt''\right). \end{aligned} \quad (\text{A7})$$

Here $\mathbf{v}[\mathbf{k}(t)] = (1/\hbar) \nabla_{\mathbf{K}} \varepsilon_{n_0}(\mathbf{K})|_{\mathbf{k}(t)}$ is the instantaneous velocity of the Bloch electron confined to the band “ n_0 ,” $D = -i\sqrt{2\pi\alpha}/V$, and $(\delta_{n_{\mathbf{q}', j'}, n_{\mathbf{q}', j'}^0 \pm 1}; \{\delta_{n_{\mathbf{q}, j}, n_{\mathbf{q}, j}^0}\}) \equiv \delta_{n_{\mathbf{q}', j'}, n_{\mathbf{q}', j'}^0 \pm 1} \prod_{\mathbf{q}, j \neq \mathbf{q}', j'} \delta_{n_{\mathbf{q}, j}, n_{\mathbf{q}, j}^0}$.

Using these results and Eq. (A5), we can easily calculate $|A_{\{n_{\mathbf{q},j}\}}^{(1)}(\mathbf{k}, t)|^2$. When calculating the double sum $\sum_{\mathbf{q}_1, j_1} \sum_{\mathbf{q}_2, j_2} (\dots)$, we make use of the relationships resulting from properties of the Kronecker delta symbol. Then the crossing terms vanish $A_{\{n_{\mathbf{q},j}\}}^{(a)*}(\mathbf{k}, t) A_{\{n_{\mathbf{q},j}\}}^{(e)}(\mathbf{k}, t) = A_{\{n_{\mathbf{q},j}\}}^{(a)}(\mathbf{k}, t) A_{\{n_{\mathbf{q},j}\}}^{(e)*}(\mathbf{k}, t) = 0$. Thus, we obtain

$$|A_{\{n_{\mathbf{q},j}\}}^{(1)}(\mathbf{k}, t)|^2 = |A_{\{n_{\mathbf{q},j}\}}^{(a)}(\mathbf{k}, t)|^2 + |A_{\{n_{\mathbf{q},j}\}}^{(e)}(\mathbf{k}, t)|^2, \quad (\text{A8})$$

where

$$\begin{aligned} |A_{\{n_{\mathbf{q},j}\}}^{(a)}(\mathbf{k}, t)|^2 = & \alpha \frac{2\pi}{V} \sum_{\mathbf{q}', j'} n_{\mathbf{q}', j'}^0 (\delta_{n_{\mathbf{q}', j'}, n_{\mathbf{q}', j'}^0 - 1}; \{\delta_{n_{\mathbf{q}, j}, n_{\mathbf{q}, j}^0}\}) \delta_{\mathbf{k}_0, \mathbf{k} - \mathbf{q}'} \\ & \times \left| \frac{\hat{\mathbf{e}}_{\mathbf{q}', j'}}{\sqrt{q'}} \cdot \int_{t_0}^t dt' \mathbf{v}[\mathbf{k}(t')] \right. \\ & \left. \times \exp\left(-\frac{i}{\hbar} \int_{t_0}^{t'} \{\varepsilon_{n_0}[\mathbf{k}_0(t'')] - \varepsilon_{n_0}[\mathbf{k}(t'')] \right. \right. \end{aligned}$$

$$\left. \left. + \hbar \omega_{q'}\} dt''\right) \right|^2 \quad (\text{A9})$$

and

$$\begin{aligned} |A_{\{n_{\mathbf{q},j}\}}^{(e)}(\mathbf{k}, t)|^2 = & \alpha \frac{2\pi}{V} \sum_{\mathbf{q}', j'} (n_{\mathbf{q}', j'}^0 + 1) (\delta_{n_{\mathbf{q}', j'}, n_{\mathbf{q}', j'}^0 + 1}; \{\delta_{n_{\mathbf{q}, j}, n_{\mathbf{q}, j}^0}\}) \\ & \times \delta_{\mathbf{k}_0, \mathbf{k} + \mathbf{q}'} \left| \frac{\hat{\mathbf{e}}_{\mathbf{q}', j'}}{\sqrt{q'}} \cdot \int_{t_0}^t dt' \mathbf{v}[\mathbf{k}(t')] \right. \\ & \times \exp\left(-\frac{i}{\hbar} \int_{t_0}^{t'} [\varepsilon_{n_0}[\mathbf{k}_0(t'')] \right. \\ & \left. \left. - \varepsilon_{n_0}[\mathbf{k}(t'')] - \hbar \omega_{q'}] dt''\right) \right|^2. \end{aligned} \quad (\text{A10})$$

APPENDIX B: MATRIX ELEMENTS OF PERTURBATION HAMILTONIAN

Matrix elements of the perturbation Hamiltonian are calculated by substituting H_I from Eq. (7) and $\psi_{n_0\mathbf{k}(t)}$ of Eq. (10), while using the properties of the photon annihilation and creation operators, $\langle n_{\mathbf{q},j} - 1 | a_{\mathbf{q},j} | n_{\mathbf{q},j} \rangle = (n_{\mathbf{q},j})^{1/2}$ and $\langle n_{\mathbf{q},j} + 1 | a_{\mathbf{q},j}^\dagger | n_{\mathbf{q},j} \rangle = (n_{\mathbf{q},j} + 1)^{1/2}$. The result is

$$\begin{aligned} & \langle \{n_{\mathbf{q},j}\}, \psi_{n_0\mathbf{k}(t)} | H_I | \psi_{n_0\mathbf{k}'(t)}, \{n'_{\mathbf{q},j}\} \rangle \\ & = -\frac{e}{m_0c} \sqrt{\frac{2\pi\hbar c}{V}} \sum_{\mathbf{q}', j'} \frac{\hat{\mathbf{e}}_{\mathbf{q}', j'}}{\sqrt{q'}} \\ & \times \left(\sqrt{n'_{\mathbf{q}', j'}} (\delta_{n_{\mathbf{q}', j'}, n'_{\mathbf{q}', j'} - 1}; \{\delta_{n_{\mathbf{q}, j}, n'_{\mathbf{q}, j}}\}) \right. \\ & \times \int \psi_{n_0\mathbf{k}}^*(\mathbf{p} + \mathbf{p}_c) e^{i\mathbf{q}'\mathbf{r}} \psi_{n_0\mathbf{k}'} d\mathbf{r} \\ & \left. + \sqrt{n'_{\mathbf{q}', j'} + 1} (\delta_{n_{\mathbf{q}', j'}, n'_{\mathbf{q}', j'} + 1}; \{\delta_{n_{\mathbf{q}, j}, n'_{\mathbf{q}, j}}\}) \right. \\ & \left. \times \int \psi_{n_0\mathbf{k}}^*(\mathbf{p} + \mathbf{p}_c) e^{-i\mathbf{q}'\mathbf{r}} \psi_{n_0\mathbf{k}'} d\mathbf{r} \right). \end{aligned} \quad (\text{B1})$$

In using $\psi_{n_0\mathbf{k}(t)}$ of Eq. (10), the first integral is equal to zero, except when $\mathbf{K}' - \mathbf{K} + \mathbf{q} = \mathbf{G}$, where \mathbf{G} is the vector of the reciprocal lattice (Here we omit, for brevity, the prime on the \mathbf{q} vector). For values of \mathbf{K} and \mathbf{q} in the first BZ, we can take $\mathbf{G} = 0$. Then, it follows that $\mathbf{K}' = \mathbf{K} - \mathbf{q}$, and since $\mathbf{k}(t) = \mathbf{K} + \mathbf{p}_c(t)/\hbar$, then we get $\mathbf{k}' = \mathbf{k} - \mathbf{q}$. In this case, we have, for the first integral in (B1),

$$\begin{aligned} I_{\mathbf{k}, \mathbf{k}'}^{(+)} & \equiv \int \psi_{n_0\mathbf{k}}^*(\mathbf{p} + \mathbf{p}_c) e^{i\mathbf{q}\mathbf{r}} \psi_{n_0\mathbf{k}'} d\mathbf{r} \\ & = \delta_{\mathbf{k}', \mathbf{k} - \mathbf{q}} \int (e^{i\mathbf{K}\mathbf{r}_0} u_{n_0\mathbf{k}})^*(\mathbf{p} + \mathbf{p}_c) e^{i\mathbf{K}\mathbf{r}_0} u_{n_0\mathbf{k} - \mathbf{q}} d\mathbf{r}_0, \end{aligned} \quad (\text{B2})$$

where the integration over $d\mathbf{r}_0$ is carried out over the primi-

tive cell volume. In the long-wavelength limit ($qa \ll 1$), $I_{\mathbf{k},\mathbf{k}'}^{(+)}$ can be approximated as

$$\begin{aligned} I_{\mathbf{k},\mathbf{k}'}^{(+)} &= \delta_{\mathbf{k}',\mathbf{k}-\mathbf{q}} \int (e^{i\mathbf{K}r_0} u_{n_0\mathbf{k}})^*(\mathbf{p} + \mathbf{p}_c) e^{i\mathbf{K}r_0} u_{n_0\mathbf{k}} d\mathbf{r}_0 \\ &= \delta_{\mathbf{k}',\mathbf{k}-\mathbf{q}} \int \psi_{n_0\mathbf{k}}^*(\mathbf{p} + \mathbf{p}_c) \psi_{n_0\mathbf{k}} d\mathbf{r}. \end{aligned} \quad (\text{B3})$$

In noting that the well-known momentum²⁴ expectation value for Bloch states is

$$\int (e^{i\mathbf{k}(t)r} u_{n_0\mathbf{k}})^* \mathbf{p} (e^{i\mathbf{k}(t)r} u_{n_0\mathbf{k}}) d\mathbf{r} = m_0 \mathbf{v}[\mathbf{k}(t)], \quad (\text{B4})$$

where $\mathbf{v}(\mathbf{k}) = (1/\hbar) \nabla_{\mathbf{k}} \varepsilon_{n_0}(\mathbf{k})$, it then follows, for $\mathbf{k}(t) = \mathbf{K} + \mathbf{p}_c(t)/\hbar$ in Eq. (B4), that

$$\int \psi_{n_0\mathbf{k}}^*(\mathbf{p} + \mathbf{p}_c) \psi_{n_0\mathbf{k}} d\mathbf{r} = m_0 \mathbf{v}(\mathbf{k}), \quad (\text{B5})$$

where $\psi_{n_0\mathbf{k}}$ are the instantaneous eigenstates of Eq. (10). Thus, Eqs. (B3)–(B5) become

$$I_{\mathbf{k},\mathbf{k}'}^{(+)} = \delta_{\mathbf{k}',\mathbf{k}-\mathbf{q}} m_0 \mathbf{v}(\mathbf{k}). \quad (\text{B6})$$

Similarly, for the second integral in Eq. (B1), one finds that

$$I_{\mathbf{k},\mathbf{k}'}^{(-)} \equiv \int \psi_{n_0\mathbf{k}}^*(\mathbf{p} + \mathbf{p}_c) e^{-i\mathbf{q}r} \psi_{n_0\mathbf{k}'} d\mathbf{r} = \delta_{\mathbf{k}',\mathbf{k}+\mathbf{q}} m_0 \mathbf{v}(\mathbf{k}). \quad (\text{B7})$$

Then, using (B1), (B6), and (B7), the matrix elements for the perturbing Hamiltonian, H_I , are established for use in Eq. (A4).

*Also with Department of Theoretical Physics, Institute for Semiconductor Physics, Pr. Nauki 41, Kiev 03028, Ukraine.

[†]Research conducted while enrolled in the Ph.D. program at NCSU.

¹F. Bloch, *Z. Phys.* **52**, 555 (1928).

²C. Zener, *Proc. R. Soc. London, Ser. A* **145**, 523 (1934).

³G. H. Wannier, *Phys. Rev.* **117**, 432 (1960); *Rev. Mod. Phys.* **34**, 645 (1962); H. M. James, *Phys. Rev.* **76**, 1611 (1949).

⁴L. Esaki and R. Tsu, *IBM J. Res. Dev.* **14**, 61 (1970).

⁵A. Sibille, J. F. Palmier, H. Wang, and F. Mollot, *Phys. Rev. Lett.* **64**, 52 (1990).

⁶For a review see, for example, K. Leo, *Semicond. Sci. Technol.* **13**, 249 (1998).

⁷Y. Shimada, K. Hirakawa, M. Odnobliouov, and K. A. Chao, *Phys. Rev. Lett.* **90**, 046806 (2003).

⁸K. Unterrainer, B. J. Keay, M. C. Wanke, S. J. Allen, D. Leonard, G. Medeiros-Ribeiro, U. Bhattacharya, and M. J. W. Rodwell, *Phys. Rev. Lett.* **76**, 2973 (1996).

⁹S. Vinnerl, E. Schomburg, S. Brandl, O. Kus, K. F. Renk, M. C. Wanke, S. J. Allen, A. A. Ignatov, V. Ustinov, A. Zhukov, and P. S. Kop'ev, *Appl. Phys. Lett.* **77**, 1259 (2000).

¹⁰T. Dekorsy, A. Bartels, H. Kurz, K. Köhler, R. Hey, and K. Ploog, *Phys. Rev. Lett.* **85**, 1080 (2000); T. Dekorsy, A. Bartels, H. Kurz, A. W. Ghosh, L. Jönsson, J. W. Wilkins, K. Köhler, R. Hey, and K. Ploog, *Physica E (Amsterdam)* **7**, 279 (2000).

¹¹A. W. Ghosh, L. Jönsson, and J. W. Wilkins, *Phys. Rev. Lett.* **85**, 1084 (2000).

¹²In *Spontaneous Emission and Laser Oscillation in Microcavities*, edited by H. Yokoyama and K. Ujihara (CRC Press, Boca Raton, 1995).

¹³E. Yablonovitch, *Phys. Rev. Lett.* **58**, 2059 (1987).

¹⁴P. G. Savvidis, B. Kolasa, G. Lee, and S. J. Allen, *Phys. Rev. Lett.* **92**, 196802 (2004).

¹⁵(a) J. B. Krieger and G. J. Iafrate, *Phys. Rev. B* **33**, 5494 (1986); (b) G. J. Iafrate and J. B. Krieger, *ibid.* **40**, 6144 (1989).

¹⁶J. Singh, *Quantum Mechanics: Fundamentals and Applications to Technology* (Wiley-Interscience, New York, 1997), p. 337.

¹⁷The term proportional to A_r^2 is of higher order of magnitude in comparison with $H_I \sim A_r$ on the small parameter $eA_r/(cp)$

$\approx [\alpha a^2 \lambda / (\pi^2 V)]^{1/2} \ll 1$, where $\alpha = e^2 / (\hbar c)$ is the fine structure constant, and $\lambda = 2\pi/q$ is the radiation mode wavelength.

¹⁸For nearest-neighbor tight binding, where $\varepsilon_{n_0}(\mathbf{K})$ can be written in the form $\varepsilon_{n_0}(\mathbf{K}) = \varepsilon_1(K_x) + \varepsilon_2(K_y) + \varepsilon_3(K_z) + \varepsilon_{n_0}(0)$; then $\mathbf{v}_{\perp}(\mathbf{K}) = (1/\hbar) [\mathbf{i}(\partial/\partial K_x) \varepsilon_1 + \hat{\mathbf{j}}(\partial/\partial K_y) \varepsilon_2]$, and therefore in keeping with Eq. (24), $\bar{\mathbf{v}}_{\perp}(\mathbf{K}_{\perp}) = \mathbf{v}_{\perp}(\mathbf{K}_{\perp})$.

¹⁹For $\omega_q = cq$, this corresponds to neglecting a small term $\sim v_{\perp}/c$ as compared to unity.

²⁰E. Schomburg, T. Blomeier, K. Hofbeck, J. Grenzer, S. Brandl, I. Lingott, A. A. Ignatov, K. F. Renk, D. G. Pavel'ev, Yu. Koschurinov, B. Ya. Melzer, V. M. Ustinov, S. V. Ivanov, A. Zhukov, and P. S. Kop'ev, *Phys. Rev. B* **58**, 4035 (1998).

²¹A. M. Bouchard and M. Luban, *Phys. Rev. B* **47**, 6815 (1993).

²²For fields much higher than $E = 10$ kV/cm, many Bloch oscillations are sustained before Zener tunneling is incurred [for example, see Ref. 15(a), where at $E = 10^3$ kV/cm, $NP_{n,n'} \ll 1$, where $P_{n,n'} \approx 10^{-17}$ is the Zener tunneling matrix element for GaAs; also, from Ref. 23, for GaAs SLs $P_{n,n'}$ scales down to $P_{n,n'} \approx 10^{-13}$ at comparable fields]; therefore, using $N = 100$ is certainly within the scope of the perturbation theory analysis employed in this paper.

²³G. J. Iafrate, J. P. Reynolds, J. He, and J. B. Krieger, *Int. J. High Speed Electron. Syst.* **9**, 223 (1998).

²⁴C. Kittel, *Quantum Theory of Solids* (Wiley and Sons, copyright: 1963, 1987), 2nd revised printing, ISBN 0-471-62412-8, p. 185, Eq. (49) therein.

²⁵F. Wolter, R. Martini, S. Tolk, P. Haring Bolivar, H. Kurz, R. Hey, and H. T. Grahn, *Superlattices Microstruct.* **26**, 93 (1999).

²⁶G. von Plessen, T. Meier, J. Feldmann, E. O. Göbel, P. Thomas, K. W. Goossen, J. M. Kuo, and R. F. Kopf, *Phys. Rev. B* **49**, 14058 (1994).

²⁷N. Sekine, Y. Shimada, and K. Hirakawa, *Appl. Phys. Lett.* **83**, 4794 (2003).

²⁸J. B. Krieger, A. A. Kiselev, and G. J. Iafrate, *Phys. Rev. B* **72**, 195201 (2005).